Stem Cell Reports
Article

ISSCR

OPEN ACCESS

Meso-Endothelial Bipotent Progenitors from Human Placenta Display Distinct Molecular and Cellular Identity

Abbas Shafiee,[1,2,3] Jatin Patel,[1,3] Dietmar W. Hutmacher,[2] Nicholas M. Fisk,[1,4,5] and Kiarash Khosrotehrani[1,3,*]

[1]UQ Centre for Clinical Research, The University of Queensland, Brisbane, QLD, Australia
[2]Institute of Health and Biomedical Innovation, Queensland University of Technology, Brisbane, QLD, Australia
[3]UQ Diamantina Institute, Translational Research Institute, The University of Queensland, Brisbane, QLD, Australia
[4]Faculty of Medicine, UNSW, Sydney, NSW, Australia
[5]Centre for Advanced Prenatal Care, Royal Brisbane & Women's Hospital, Brisbane, QLD, Australia
*Correspondence: k.khosrotehrani@uq.edu.au
https://doi.org/10.1016/j.stemcr.2018.01.011

SUMMARY

The existence of bipotential precursors for both mesenchymal and endothelial stem/progenitor cells in human postnatal life is debated. Here, we hypothesized that such progenitors are present within the human term placenta. From a heterogeneous placental single-cell suspension, a directly flow-sorted $CD45^{-}CD34^{+}CD144^{+}CD31Lo$ population uniquely differentiated into both endothelial and mesenchymal colonies in limiting dilution culture assays. Of interest, these bipotent cells were in vessel walls but not in contact with the circulation. RNA sequencing and functional analysis demonstrated that Notch signaling was a key driver for endothelial and bipotential progenitor function. In contrast, the formation of mesenchymal cells from the bipotential population was not affected by TGFβ receptor inhibition, a classical pathway for endothelial-mesenchymal transition. This study reveals a bipotent progenitor phenotype in the human placenta at the cellular and molecular levels, giving rise to endothelial and mesenchymal cells *ex vivo*.

INTRODUCTION

Vascularization is an essential physiological process that occurs during embryonic and fetal development and in disease (Carmeliet, 2000). It is well documented that endothelial cells arise from precursors (Minasi et al., 2002; Vodyanik et al., 2010) of the splanchnopleural or paraxial mesoderm (Pardanaud et al., 1996). Among mesodermal cells, hemangioblasts that differentiate into both hematopoietic and endothelial cells (Choi et al., 1998; Hirschi, 2012) have received much attention, but they are spatially restricted to the periphery of the endoderm as well as the aorta-gonad-mesonephros region at later stages of development (Dzierzak and Speck, 2008). Therefore, endothelial cells would be expected to also derive from mesodermal progenitors devoid of hematopoietic potential.

Recently, Vodyanik et al. (2010) proposed the existence of a mesoderm-derived bipotent progenitor cell, the so-called mesenchymoangioblast, which could be derived and characterized from embryonic stem cells. Although hemangioblast and hemogenic endothelium have been broadly characterized during development (reviewed in Choi et al., 1998), precursors for mesenchymoangioblasts with both endothelial and mesenchymal potential have seldom been explored *in vivo*. In this regard, Bianco and Cossu (1999) identified vessel-associated progenitors, "mesoangioblasts," with potential to form both vessel and associated cells in murine models. Mesoangioblasts isolated from dorsal aorta at embryonic day 9.5 demonstrated extensive self-renewal capacity with the potential to form most mesodermal lineages on transplantation (Minasi et al., 2002). Moreover, given the similarity of their surface marker profile with mesenchymal stem cells (MSCs), mesoangioblasts were proposed as the ancestors of postnatal MSCs (Jiang et al., 2002; Minasi et al., 2002; Pittenger et al., 1999). Murine experiments reported expression of Flk1 (vascular endothelial growth factor receptor 2) (Cossu and Bianco, 2003), CD34, or c-Kit (Minasi et al., 2002) in mesoangioblasts. The existence of mesoangioblasts in postnatal life has also been suggested through isolation from muscle pericytes (Bonfanti et al., 2015). Others have reported mesodermal precursors with endothelial capacity in bone marrow (Reyes et al., 2002; Roobrouck et al., 2011). Despite these various indications in essentially murine studies, the existence of a bipotential population with capacity to give rise to mesenchymal and endothelial progeny in human tissues remains questioned.

The recent description of a functional hierarchy in the endothelium based on colony-formation capacity and proliferative potential has allowed to define progenitors, namely highly proliferative endothelial colony-forming cells (ECFCs) as opposed to low proliferative potential ECFCs or endothelial clusters (Ingram et al., 2004). Our group recently demonstrated *in vivo* the heterogeneity and hierarchy of the endothelial compartment in murine vasculature, allowing a functional definition of endothelial progenitors (Patel et al., 2016a). We have also demonstrated that human ECFCs as well as human MSCs of fetal origin can be isolated from the term placenta (Patel et al.,

2013, 2014). Here, we hypothesized that vascularization of the human placenta from mesodermal precursors gives a unique opportunity to prospectively characterize the human mesoangioblast phenotype. Our findings support the existence *in vivo* of meso-endothelial bipotent progenitors capable of giving rise to both endothelial and mesenchymal progeny. Characterization of this progenitor distinguishes it from both mesenchymal (MSCs) and endothelial progenitors (ECFCs) at the functional and molecular level.

RESULTS

Placental EPCs Are Enriched in the CD45$^-$CD34$^+$ Population

To evaluate progenitors that would give rise to endothelial cells *in vivo* (called herein EPCs, i.e., endothelial progenitor cells) and able to form highly proliferative colonies in culture (HPP-ECFCs), we adopted a systematic and prospective isolation and culturing strategy. When unsorted term placental cells were cultured in EGM2, this resulted in both mesenchymal (Figure S1A) and endothelial cells (Figure S1B) before passaging. Only 0.011% ± 0.001% of placental cells could form proliferative colonies, and from this only 0.00066% ± 0.0001% were HPP-ECFCs (Figure S1C). Flow cytometry also confirmed that 12.4% ± 3.9% of unsorted placental cells expressed CD31 at primary culture (Figure S1D). Upon passaging and persistent culture, endothelial cells were rapidly outgrown by mesenchymal cells (probably of maternal origin [Patel et al., 2014]) with a fibroblastic morphology, expressing MSC surface markers (data not shown).

To enrich for EPCs or bipotential cells with endothelial potential, we next characterized term placental cells according to well-established endothelial (CD31 and CD34) and hematopoietic (CD45) surface markers (Figures 1A and 1B). Unsorted placental cells consisted mostly of hematopoietic (CD45$^+$) cells and comprised a small CD34$^+$ fraction.

Upon digestion and single-cell suspension, we used magnetic activated cell sorting (MACS) sorting to isolate and test the colony-forming capacity of different cell fractions (Figure 1A). Sorting CD45$^-$CD34$^+$ cells enriched for endothelial potential as the number of HPP-ECFCs in this population was superior to those in the CD45$^-$ and the CD45$^-$CD34$^-$ populations (Figure 1B). CD34$^+$ cells represented a small population of unsorted placental cells (7.9% ± 3.6%), and CD45$^-$CD34$^+$ represented a fraction of that (3.0% ± 1.2%) (Figure 1C, n = 10 placentas). However, not all the cells in CD45$^-$CD34$^+$ showed an endothelial phenotype. In some cultures a significant mesenchymal population still overtook endothelial cells, suggesting that a mesenchymal progenitor could be found in the CD45$^-$CD34$^+$ population.

Fetal EPCs and MSCs Purified Based on CD31 Expression Levels among CD45$^-$CD34$^+$ Placental Cells

To further purify endothelial from mesenchymal cells in CD45$^-$CD34$^+$ cells, we made use of the endothelial cell surface antigen CD31 (*PECAM-1*).

Based on CD31 levels, the CD45$^-$CD34$^+$ cells could be divided into four populations (Figures 1D and 1E). Fluorescence minus one (FMO) analysis clearly showed that one population was CD31 negative (CD31Neg) and included 24.8% ± 10.4% of CD45$^-$CD34$^+$, while the three other populations expressed low (CD31Lo), intermediate (CD31Int), and high (CD31Hi) levels of CD31, and included 20.7% ± 3.9%, 25.7% ± 5.6%, and 28.8% ± 8.2% of CD45$^-$CD34$^+$ cells, respectively (Figures 1D–1F). We employed a cell-sorting strategy directly from the digested term placenta and cultured these four populations individually in EGM2 to explore their potency (Figure 1G). Extreme care was taken to reduce the gating width to avoid any overlap in CD31 levels. All fractions expressed CD34 at a high level and were CD45 negative as verified by isotype control, FMO analysis, and RT-PCR (data not shown). Fetal origin of all cells in the CD45$^-$CD34$^+$ population was confirmed by fluorescence *in situ* hybridization and genomic PCR analysis (data not shown). The percentage of each subpopulation at each step of sorting was calculated using flow cytometry. In comparison with unsorted placenta, the percentage of CD45$^-$CD34$^+$ population was increased 16- and 647-fold after CD45$^+$ depletion and CD45$^+$ depletion and CD34$^+$ MACS enrichment, respectively (Figure S2A). The subpopulations based on CD31 levels represented only 0.005%–0.025% of placental populations after CD45$^+$ depletion (Figure S2B). These populations were enriched further after CD45$^+$ depletion and CD34$^+$ magnetic selection, reaching 0.8%–1% of total cells (Figure S2C).

Among the CD45$^-$CD34$^+$ cells, CD31Lo cells formed 336.9 ± 126.0 colonies per 1 × 10^6 seeded cells (mean ± SD, Figures 1G and 1I). This was significantly lower compared with all other CD34$^+$ populations. CD31Neg cells resulted in pure mesenchymal colonies (Figures 1G and 1H), while pure endothelial colonies were derived from CD31Int and CD31Hi populations (Figures 1G, 1J, and 1K). CD31Neg cells never gave rise to endothelial colonies and, similarly, CD31Int and CD31Hi cells never gave rise to mesenchymal colonies (conclusive results from >30 placental cell cultures). Further examination identified the HPP-ECFCs to derive almost exclusively from the CD31Int population, and only colonies emanating from the CD31Int population could be further passaged and expanded as expected from ECFCs (Yoder, 2010). The CD31Hi cells gave rise to mature endothelial clusters with

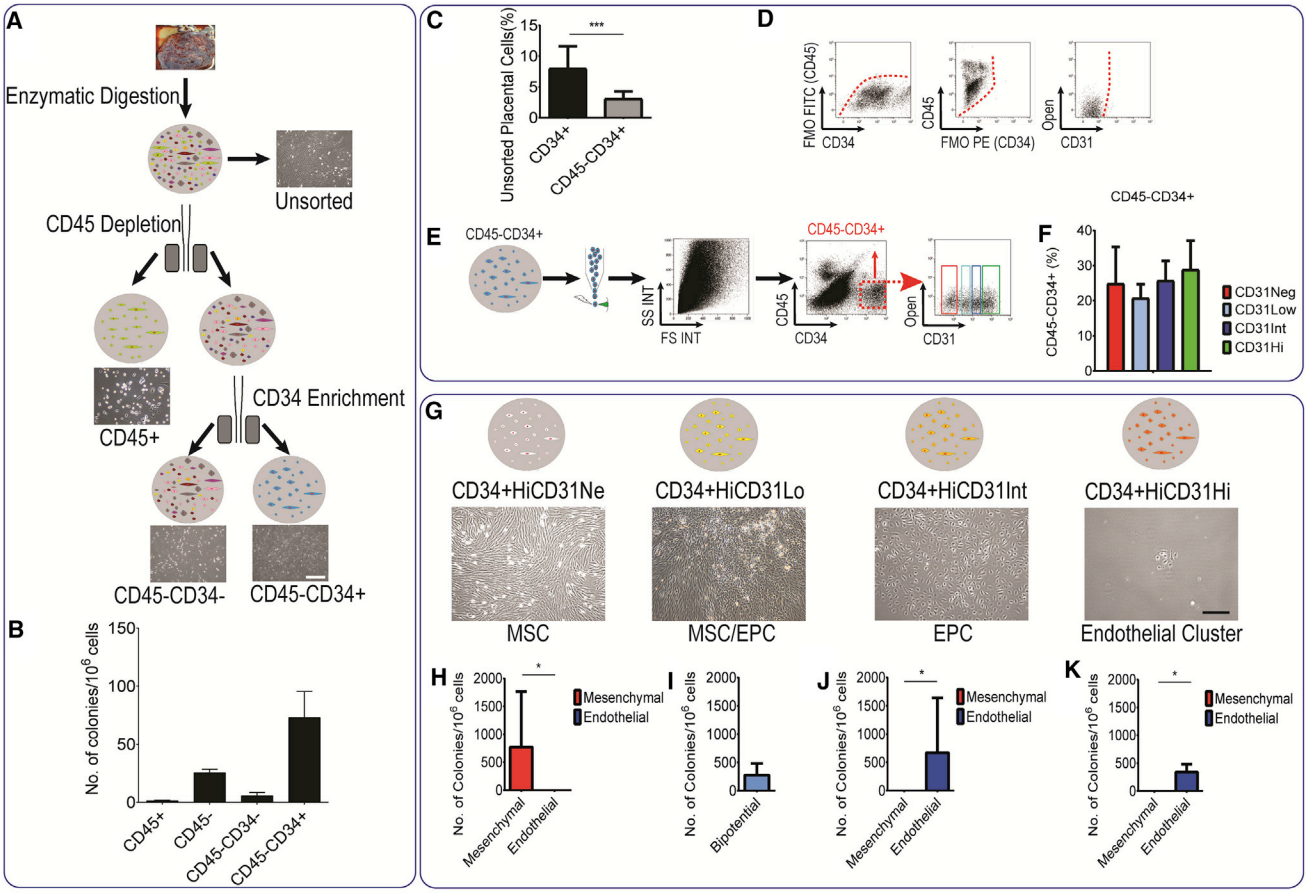

Figure 1. Placental Endothelial Progenitor Cells Are Enriched in the CD45$^-$CD34$^+$ Population

(A) To enrich the endothelial colony-forming cell (ECFC) population, we enriched placental cells for CD45$^-$CD34$^+$ cells.

(B) Number of HPP-ECFCs forming cobblestone-like endothelial colonies in this population was superior to the CD45$^-$ and the CD45$^-$CD34$^-$ populations (data presented as mean ± SD).

(C) Flow cytometry on placental unsorted cells showing frequency of CD34$^+$ or CD34$^+$CD45$^-$ cells. To further purify EPC we devised a sorting strategy.

(D and E) Four different populations were observed based on CD31 levels in CD45$^-$CD34$^+$ population. Fluorescence minus one analysis (D) demonstrated that (E) one population is CD31 negative, while the three other populations express low, intermediate, and high levels of CD31.

(F) Percentage of each population (data presented as mean ± SD).

(G–K) CD31Neg cells resulted in pure mesenchymal stem cell (MSC) colonies. Pure endothelial cells were derived from CD31Int and CD31Hi populations; upon culture, CD31Int and CD31Hi cells never formed mesenchymal colonies. EPCs were to be almost exclusively in the CD31Int population. For CD31Low population the number of bipotential colonies is presented (data presented as median with interquartile range). Scale bar, 100 μm.

*$p < 0.05$ and ***$p < 0.005$.

limited proliferative potential. The detailed characterization of the progeny of CD31Neg cells (Patel et al., 2014) has been reported by us recently. In brief, CD31Neg cells once expanded in culture had the morphology, cell surface antigens, and differentiation potential of MSCs (Patel et al., 2014). On the other hand, colonies derived from CD31Int cells had cell surface antigens, gene expression, proliferation, and vasculogenic potential identical to that already described in cord-blood ECFCs (Ingram et al., 2004; Patel et al., 2013). Overall, it seemed that by using three simple cell surface markers, EPCs and mesenchymal progenitors giving rise to fetal HPP-ECFCs and fetal MSCs, respectively, could be identified.

CD45$^-$CD34$^+$ CD31Lo Cells Give Rise to Mesenchymal and Endothelial Colonies

Of interest, the CD31Lo population contained individual colonies with mixed morphologies of endothelial and

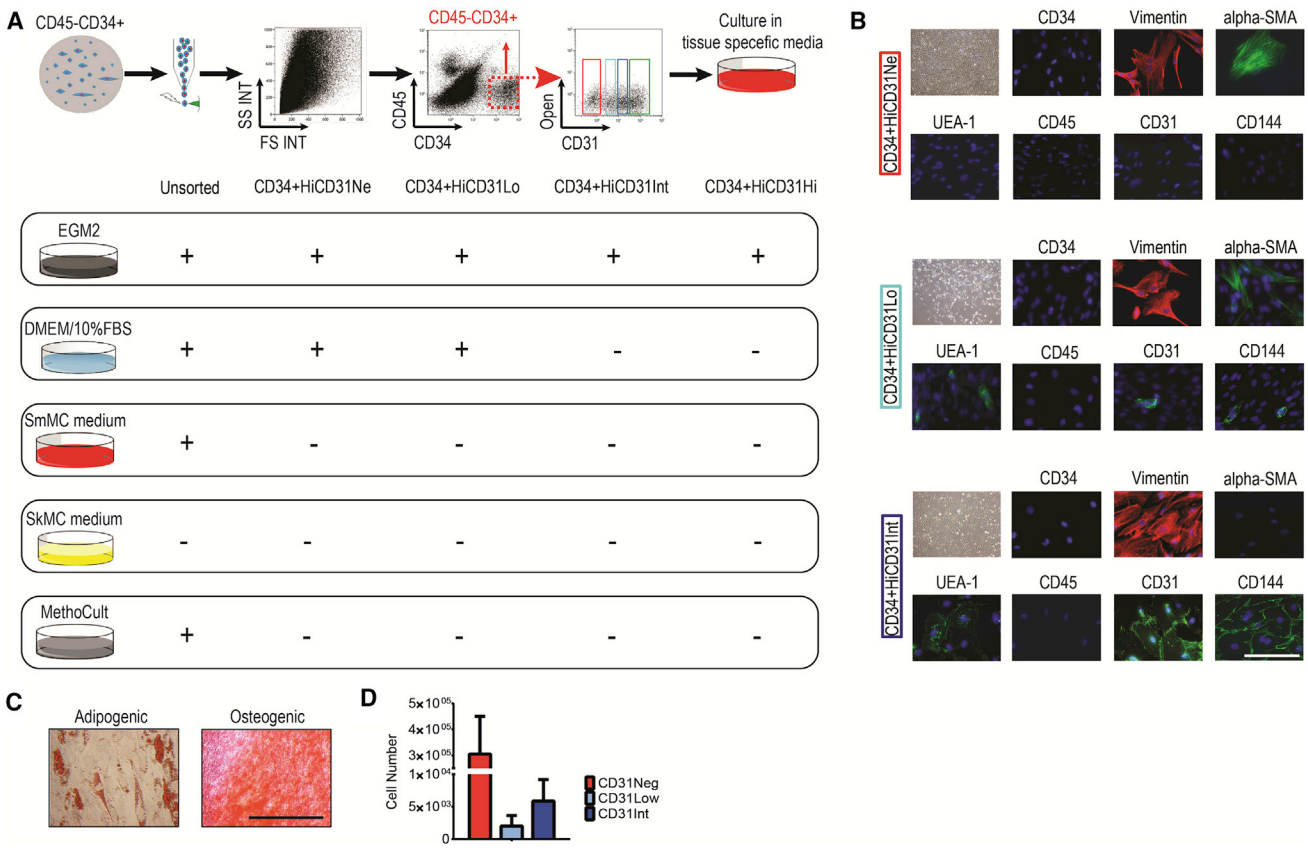

Figure 2. CD45$^-$CD34$^+$ CD31Lo Population Demonstrated Bipotential Characteristics

(A) Placenta-derived cells were cultured in different media for 2–3 weeks, DMEM supplemented with 10% fetal bovine serum (a standard mesenchymal stem cell [MSC] growth medium), endothelial growth medium (EGM2, a standard endothelial growth medium), skeletal and smooth muscle cell media, and MethoCult (a standard hematopoietic medium). None of CD45$^-$CD34$^+$ subpopulations could grow in smooth and skeletal muscle media, or displayed hematopoietic capacity. CD31Neg and CD31Lo cells gave rise to colonies in standard MSC growth medium.

(B) *In vitro* characterization of each population cultured in EGM2 using immunofluorescence at passage 2. Upper rows: CD31Neg-derived cells were negative for CD34, UEA-1, CD45, CD31, and CD144, and positive for α-SMA and vimentin. Middle rows: staining of the CD31Lo population resulted in heterogeneous cells expressing CD31, CD144, and UEA-1 in parts of the colony and α-SMA in other parts. Bottom rows: CD31Int-derived cells were negative for CD34, α-SMA, and CD45, but labeled with vimentin, UEA-1, CD31, and CD144. Scale bar, 20 μm.

(C) MSC derived from CD31Lo population on passage differentiated into adipocyte and osteoblast lineages after 2 weeks of culture in appropriate differentiation medium. Scale bar, 100 μm.

(D) Cell number in each subpopulation after culturing 10,000 fresh isolated and flow-sorted cells in EGM2 after 3 weeks (mean ± SD).

mesenchymal cells under EGM2 cell culture conditions. This unique observation led us to suspect the existence of a progenitor with bipotential capacity, and prompted us to examine the differentiation potential of the CD31Lo cells compared with the other three populations in different culture media (Figure 2A). Among all CD45$^-$CD34$^+$ populations, only CD31Neg and CD31Lo cells could give rise to colonies in DMEM supplemented with 10% fetal bovine serum (FBS), a standard MSC growth medium (Figures 2A and S3A). None of the CD45$^-$CD34$^+$ subpopulations could grow in smooth and skeletal muscle medium or displayed hematopoietic capacity (Figures 2A and S3A). Primary skeletal cells, smooth muscle cells (Figure S2B), or placental CD45$^+$ cells (Figure S3C) were used as positive control for their respective growth media.

In vitro characterization of each population at passage 2 cultured in EGM2 using immunofluorescence staining demonstrated that the CD31Neg-derived colonies were negative for CD34, UEA-1, CD45, CD31, or CD144 and homogeneously positive for vimentin and α-smooth muscle actin (α-SMA; Figure 2B). In contrast, colonies derived

from CD31Int cells were negative for CD34, α-SMA, and CD45, but homogeneously labeled with vimentin, UEA-1, CD31, and CD144 as would be expected from ECFCs (Figure 2B). The CD31Lo population gave rise to cells homogeneously negative for CD34 and CD45 and positive for vimentin. Most importantly, the colonies derived from the CD31Lo population contained some cells expressing CD31, CD144, UEA-1 while others expressed α-SMA, further supporting the capacity of the CD31Lo cells to give rise to both endothelial and mesenchymal cells within the same colony (Figure 2B). Upon further culture in EGM2 or in DMEM medium, colonies derived from the CD31Lo population gave rise to pure mesenchymal cells at P3 (data not shown). These cells could differentiate into adipocyte and osteoblast lineages after 2 weeks of culture in appropriate differentiation media (Figure 2C). Moreover, CD31Lo cells had a population doubling time of 41 ± 6 hr. Additionally, compared with other subpopulations the CD31Lo fraction produced the smallest number of progeny (Figure 2D).

Bipotential Capacity of CD45$^-$CD34$^+$ CD31Lo Cells in Limiting Dilution Assay

Generating Single Colonies in Limiting Dilution

To further confirm the bipotency of CD31Lo cells, it was essential to ensure that only single colonies were analyzed and that our observations were not the result of contaminating cells from the CD31Neg or CD31Int populations. Given our reproducible rates of colony formation for each of the CD45$^-$CD34$^+$ populations, it was expected that only 1 out of every 1,000 cells would give rise to a colony. To ensure that isolated colonies were derived from single cells, we gated and sorted freshly isolated placental CD45$^-$CD34$^+$ cells based on CD31 level and cultured them in 96-well plates at 10 cells per well, 100-fold below their expected colony-forming frequency. More than 2,500 wells were prepared for each of the four separate CD45$^-$CD34$^+$ subpopulations. After 2 weeks, colonies derived from each population were evaluated under a microscope (Figure 3A). As expected, colonies emanating from CD31Neg and CD31Int cells were exclusively mesenchymal and endothelial (cobblestone shape), respectively, in morphology whereas CD31Hi derived cells only formed small clusters that could not be expanded or passaged. Passaging of individual colonies from CD31Neg and CD31Int resulted in similar types of colonies that could be characterized as mesenchymal and endothelial, respectively. This confirmed the existence of pure mesenchymal (positive for CD90, CD105, CD106, and CD146 and negative for CD31, CD45, and CD144) and pure endothelial (positive for CD31, CD34, CD144, and CD146 and negative for CD90, CD45, CD106, and CD117) progenitors in CD31Neg and CD31Int populations, respectively (Figure S4).

Seeding of CD31Lo cells resulted in fewer individual colonies compared with the other two populations (n = 3 placentas, CD31Neg: 2,772 ± 418, CD31Low: 940 ± 163, and CD31Int: 2,453 ± 410 colonies per million seeded cells, mean ± SD; Figures 3B–3D). Based on the data observed and the large numbers of empty wells, we calculated the probability of monoclonality as previously described for limiting dilution experiments (Lietzke and Unsicker, 1985). For CD31Low seeded cells, the colonies observed had a probability of 0.9996 to be monoclonal. This further ensured that the seeding of 10 cells per well is likely to result in single-cell-derived colonies.

A Self-Renewal Hierarchy among Endothelial Cells

We next focused on colonies that could be identified as HPP-EPCs. Colonies were scored as endothelial cluster (EC, <50 cells), low proliferative potential-EPC (LPP, for 50–2,000 cells), and HPP-EPCs (for >2,000 cells). Of significant interest, EPCs giving rise to HPP-ECFCs were concentrated in the CD31Int population compared with the CD31Hi population (on average 612 versus 40 HPP-ECFCs per million seeded cells, respectively; Figures 3D–3F). The CD31Int population also contains larger numbers of LPP-ECFCs (1,222 versus 300 per million seeded cells) but fewer endothelial clusters (232 versus 1,089 per million seeded cells) than the CD31Hi population (Figure 3F). Altogether, using limiting dilution assay and quantitative analysis, we suggest an endothelial hierarchy between CD31Int and CD31Hi endothelial cells *in vivo* (Figure 3G). The CD31Int cells represent an *in vivo* population that is therefore enriched with endothelial progenitors that in culture give rise to HPP-ECFCs.

Mesenchymal and Endothelial Bipotency of the CD31Lo Population

Further characterization of CD31Lo population cultured at the single-colony level in EGM2 recapitulated the heterogeneity previously observed. All cells were positive for vimentin, whereas for UEA-1, CD31, and CD144 as endothelial markers or FSP1 as a mesenchymal marker, there was heterogeneous and mutually exclusive expression in colonies presumably derived from single cells (Figure 3H). This clearly supported the capacity of the CD31Lo cells to give rise to both endothelial and mesenchymal cells within the same colony; accordingly these cells were named meso-endothelial bipotent progenitors. Microscopy further suggested derivation of cells of both endothelial and mesenchymal morphology within a single colony (from a single CD45$^-$CD34$^+$CD31Lo cell) (Figures S5A and S5B).

To confirm these bipotential features, we next passaged individual colonies presumably isolated from single CD45$^-$CD34$^+$CD31Lo cells at limited dilution and

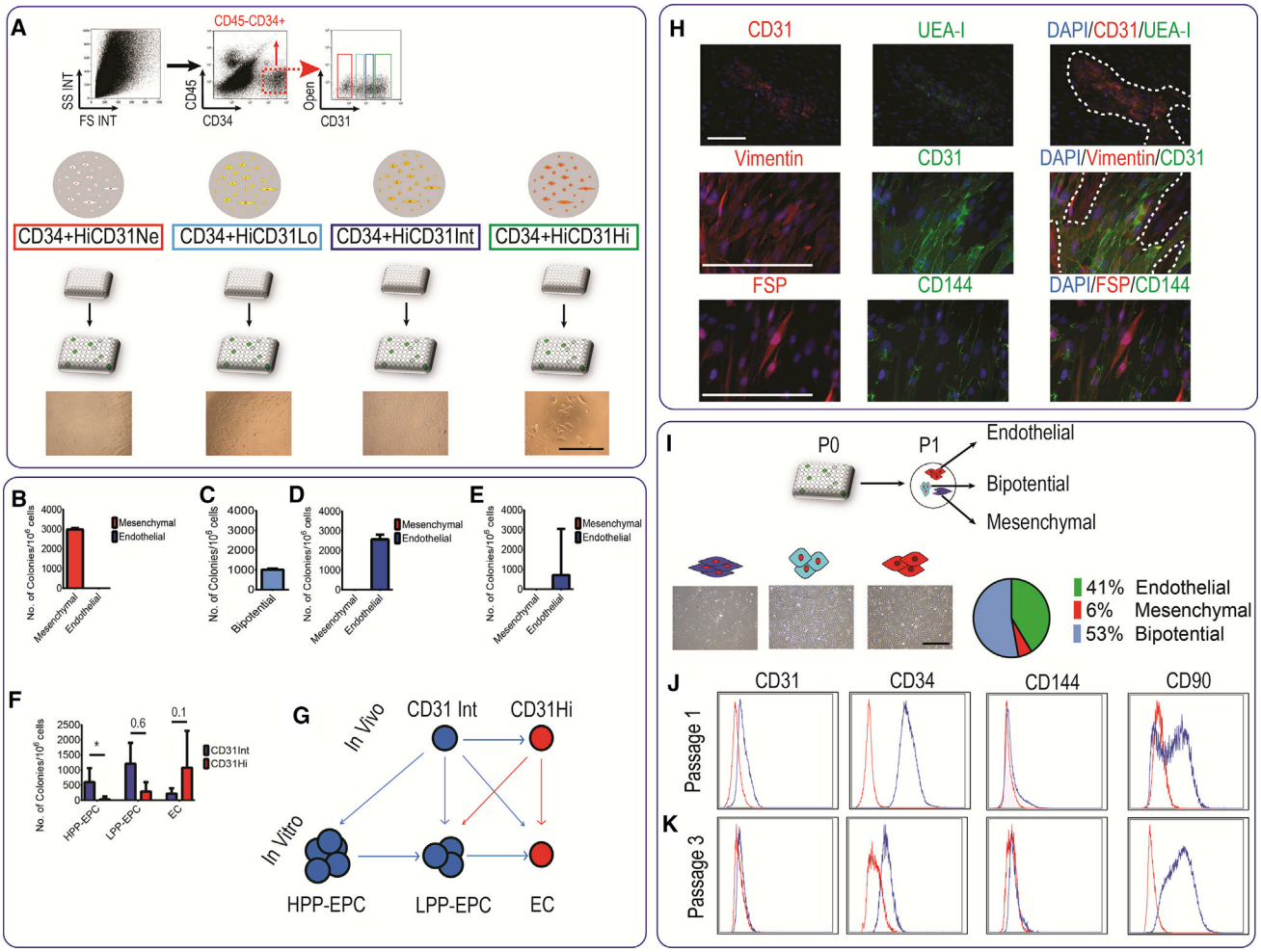

Figure 3. Bipotential Capacity of CD45$^-$CD34$^+$ CD31Lo Cells in Limiting Dilution Assay

(A) CD45$^-$CD34$^+$ cells were gated and sorted based on CD31 level, and cultured in 96-well plates at 10 cells per well; a total of more than 2,500 wells were prepared for each of the CD45$^-$CD34$^+$ subpopulations. After 2 weeks, colonies derived from each population were evaluated under the microscope. Scale bar, 100 μm.

(B–E) Number and type of colonies harvested from 1 million cells of each CD45$^-$CD34$^+$ subpopulation after 2–3 weeks. Bipotential cells contained both endothelial and mesenchymal cells (n = 3 independent placentas, data presented as median with interquartile range).

(F) Number of high proliferative potential (HPP-) and low proliferative potential (LPP-) endothelial progenitor cells (EPC), and endothelial clusters (EC) isolated from CD31Int and CD31Hi fractions.

(G) Schematic suggesting a self-renewal hierarchy among CD31Int and CD31Hi cells *in vivo* and *in vitro*.

(H) Individual colonies from CD31Lo population primary culture were stained for CD31, UEA-I, CD144, and fibroblast-specific protein (FSP). Scale bar, 100 μm.

(I) Single colonies derived from CD31Lo population were harvested and passaged and resulted in a mixture of endothelial, mesenchymal, and bipotential colonies. Quantitative analysis showed that most colonies are bipotential in passage 1. Scale bar, 100 μm.

(J and K) Flow-cytometry analysis on bipotential colonies from CD31Lo cells at passage 1 (J) and passage 3 (K).

*$p < 0.05$.

characterized them further. In this setting, 41% of resulting colonies seemed purely endothelial, 6% were purely mesenchymal, and the remaining 53% were again bipotential (Figure 3I). Although all cells were CD34 positive, flow-cytometry analysis of secondary bipotential colonies showed heterogeneity in expression of CD31 (13% ± 3% positive), CD144 (17% ± 25% positive), and CD90 (52% ± 32% positive) levels (Figure 3J); Pure endothelial and mesenchymal colonies obtained from CD31Int and CD31Neg populations expressed CD31 or CD90 in a mutually exclusive way (Figures S4A and S4B). Multicolor flow-cytometric analysis of key markers (CD31, CD34, and

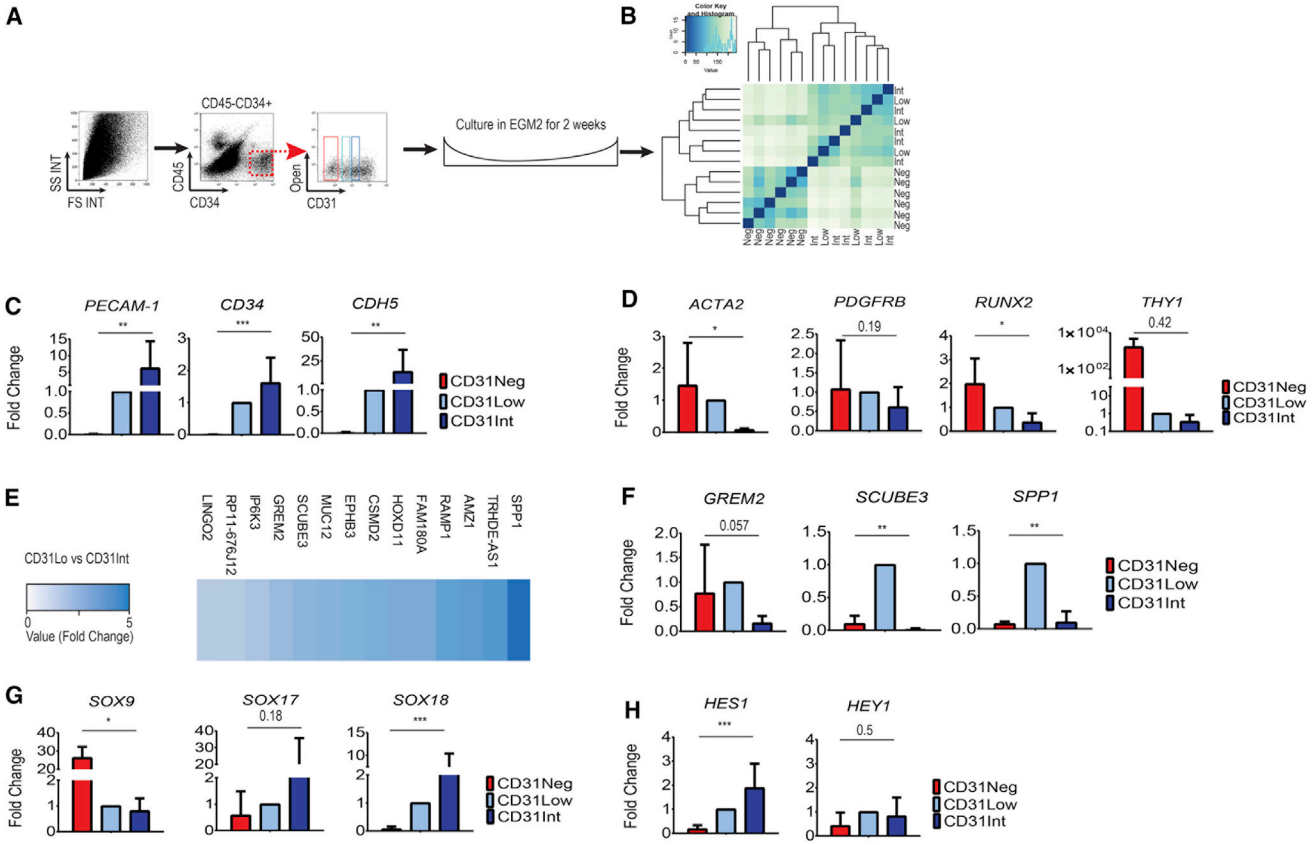

Figure 4. Meso-Endothelial Bipotent Cells Display Vascular and Mesenchymal Molecular Signature

(A) Upon sorting and short-term culture, each population was recovered before passaging and RNA extracted.

(B) Unsupervised clustering of all three populations considered together.

(C) Expression of endothelial key genes in CD31Neg, Low, and Int populations as validated using qRT-PCR.

(D) Expression analysis of pericyte and mesodermal progenitor cell key markers (*ACTA2* and *PDGFRB*, *RUNX2* and *THY1*) was assessed using qRT-PCR.

(E) Heatmap showing the comparative analysis between CD31Lo and CD31Int populations (more than 3-fold difference in RNA expression).

(F) Comparative expression was validated by qRT-PCR.

(G) Differential expression of SOX genes (*SOX9*, *SOX17*, and *SOX18*) was confirmed using qRT-PCR.

(H) Higher expression of Notch pathway target genes in CD31Lo and CD31Int populations as confirmed by qRT-PCR.

*p < 0.05, **p < 0.01, and ***p < 0.005.

CD90) showed that 75% and 24% of cells were $CD90^+$ $CD34^+$ and $CD90^-CD34^+$. Multicolor staining for CD31, CD34, and CD90 showed that 6% and 7% of cells were $CD31^+CD34^+$ and $CD31^+CD90^+$, respectively (Figure S4C).

However, further passaging resulted in populations of cells negative for endothelial markers (CD31 and CD144, Figure 3K). This confirmed that colonies could maintain such bipotency at least up to passage 1 in EGM2 medium, allowing gene expression studies at passage-0 cultures (Figure 4). The phenotype of all populations was investigated up to at least six passages, confirming that only mesenchymal cells could be detected after passage 3 through morphology but also flow cytometry (Figure 3K) and immunofluorescence (data not shown).

Bipotential Cells Display Vascular and Mesenchymal Molecular Signature

To assess the placental cell population's gene expression profile, we performed RNA sequencing on the three placental populations with high colony-forming potential. After sorting and short-term culture to gain a sufficient cell quantity, each population was recovered before passaging and subjected to RNA extraction. Unsupervised clustering distinguished CD31Neg from CD31Lo and CD31Int populations, whereas CD31Lo and Int could not be easily distinguished when all three populations were considered together (Figures 4A and 4B; Supplemental Results; Tables S5–S7; SRA accession ID: SRP127770). qRT-PCR confirmed that *PECAM-1* (725×), *CD34* (349×), and *CDH5* (1,390×)

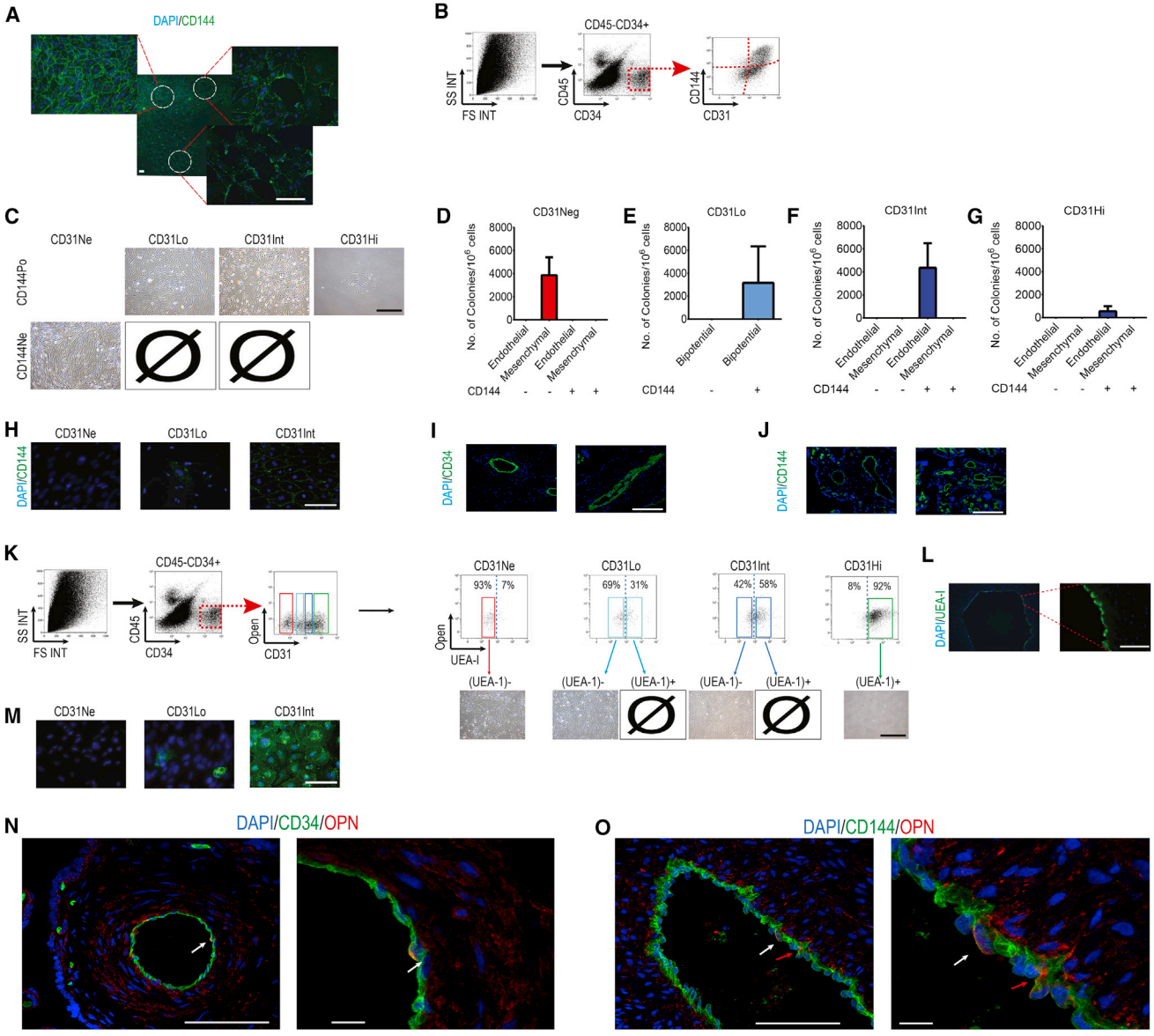

Figure 5. Meso-Endothelial Bipotent Progenitors and Endothelial Progenitor Cells Were Further Characterized Based on Level of CD144 Expression *In Vivo*

(A) CD31Lo population highly express CD144 marker at primary culture. Scale bars, 200 μm (low magnification) and 50 μm (high magnification).

(B) The $CD45^{-}CD34^{+}$ populations were examined for CD144 expression *in vivo*. CD31Lo and CD31Int cells were divided in two categories based on CD144 expression. Sorted cells were cultured in coated plates with EGM2.

(C) The CD31NegCD144Neg progenitors gave rise to mesenchymal cells. The CD31Lo bipotential progenitors were within the $CD144^{+}$ fraction. Highly proliferative EPCs were isolated from the $CD31IntCD144^{+}$ population and $CD31HiCD144^{+}$ cells formed endothelial clusters with no proliferation potential in subsequent passages. Scale bar, 100 μm.

(D–G) The use of CD144 allowed further enrichment in EPCs and bipotent progenitors.

(H) Upon *in vitro* culture and in passage 2, cells were stained with CD144 antibody and the CD31Neg population gave rise to $CD144^{-}$ cells, $CD31Lo/CD144^{+}$ population gave rise to a mixture of $CD144^{+}$ and $CD144^{-}$ cells, and $CD31Int/CD144^{+}$ ended up with $CD144^{+}$ cells. Scale bar, 50 μm.

(I and J) Representative images of placental sections stained with CD34 and CD144 antibodies. As expected, all positive cells reside in an intimal position within vascular structures. Scale bar, 100 μm.

(legend continued on next page)

genes were upregulated in CD31Int versus CD31Neg (Figure 4C, $p < 0.01$), with the expression of key endothelial genes in CD31Lo cells being lower than in the CD31Int population, *PECAM-1* (0.1×), *CD34* (0.6×), and *CDH5* (0.7×) (Figure 4C). Higher expression of MSC precursor genes (*PDGFRB*, *ACTA2*, *RUNX2*, and *THY1*) was confirmed using qRT-PCR (Figure 4D). Only the CD31Neg population could highly express pericyte key markers, chondroitin sulfate proteoglycan 4 (*CSPG4*) and *MUC12*, as confirmed by qRT-PCR (Table S4). Finally, comparative analysis between CD31Lo and CD31Int cells identified differential expression of 14 additional genes (more than 3-fold difference in expression, Figure 4E and Table S6) as confirmed using qRT-PCR, namely Gremlin 2 (*GREM2*), Signal Peptide, CUB Domain and EGF-Like Domain Containing 3 (*SCUBE3*), and Secreted Phosphoprotein 1 (*SPP1*) (Figure 4F). Of interest, our cell populations displayed differential expression of SOX genes as confirmed using qRT-PCR; while the CD31Neg population represented higher expression of *SOX9*, the CD31Lo and CD31Int components showed higher expression of *SOX17* and *SOX18* (Figure 4G). Similarly, NOTCH signaling, previously shown to maintain self-renewal in ECFCs (Patel et al., 2016b), was significantly upregulated with its target genes expressed in CD31Lo and CD31Int populations as confirmed by qRT-PCR (Figure 4H).

Meso-Endothelial Bipotent Progenitors and EPCs Are in Intimal but Subluminal Position within Blood Vessels *In Vivo*

Our gene expression findings of widespread CD144 (VE-cadherin, a classical endothelial marker and a product of the *CDH5* gene) expression in CD31Lo populations with mesenchymal potential were surprising and warranted further validation. Primary colonies at passage 0 from CD31Lo cells were immunostained with CD144 antibody and, as demonstrated in Figure 5A, all cells derived from single colonies were CD144 positive. This differed from immunostaining on established colonies (Figure 2B) where cells harboring endothelial markers were sparsely distributed.

To validate this finding, we studied the $CD45^{-}CD34^{+}$ populations *in vivo* to analyze CD144 expression. Among $CD45^{-}CD34^{+}$ cells obtained from placental cell suspensions, CD31Neg cells were CD144 negative based on FMO analysis (Figure 5B). In contrast, all CD31Hi cells were CD144 positive. However, CD31Int cells and mostly CD31Lo could be divided in two distinct categories based on CD144 expression. Therefore, six individual $CD45^{-}CD34^{+}$ populations were sorted based on CD31 and CD144 expression levels after gating on $CD45^{-}CD34^{+}$ population (Figures 5B and 5C) and cultured in EGM2. This demonstrated that the mesenchymal progenitors among the CD31Neg population were indeed CD144Neg (Figures 5C and 5D) and that the mature ECs obtained from the CD31Hi population were $CD144^{+}$ as expected (Figures 5C and 5G). Of significant interest, EPCs giving rise to HPP-ECFCs were concentrated in the $CD31IntCD144^{+}$ population, and no proliferative endothelial colony could be recovered from the CD31Int/CD144-population (Figures 5C and 5F).

Importantly, the CD31Lo meso-endothelial progenitors were also within the $CD144^{+}$ fraction and no colonies could be obtained from the $CD31LoCD144^{-}$ cells (Figures 5C and 5E). This clearly validated our gene expression observations in the CD31Lo population. On a practical note, the use of CD144 allowed a further 4.8-fold enrichment in EPCs as identified by CD31Int expression and a 9.4-fold enrichment in meso-endothelial progenitors, since 3,186 colonies per million seeded cells could be obtained in $CD45^{-}CD34^{+}CD31LoCD144^{+}$ (compared with 336 colonies [Figure 1I] if using $CD45^{-}CD34^{+}CD31Lo$ alone) (Figure 5E).

Upon culture, the $CD31Lo/CD144^{+}$ population gave rise to a mixture of $CD144^{+}$ and $CD144^{-}$ cells in established colonies and displayed the two mesenchymal and endothelial morphologies (Figure 5H). However, after three passages CD144 expression was lost in parallel with the progression of cultures toward a mesenchymal phenotype. This suggested that *in vivo*, both EPCs and bipotent progenitors are CD144 positive. We therefore stained placental sections for CD144 and observed, as expected, that all

(K) Placental arteries were firstly washed with PBS and then perfused with FITC-conjugated *Ulex europaeus* agglutinin I (UEA-I) and a single-cell suspension prepared. The single-cell suspension was stained with antibodies and sorted. On sorting, almost all CD31Neg cells were UEA-I negative, and CD31Hi cells were entirely UEA-I positive. However, CD31Lo and CD31Int populations had UEA-I-positive and -negative fractions.

(L) Placental sections stained with UEA-I antibody; all $(UEA\text{-}I)^{+}$ cells reside in intimal position within vascular structures. Scale bar, 50 μm.

(M) Upon *in vitro* culture and in passage 2, the CD31Neg population gave rise to $(UEA\text{-}I)^{-}$ cells; however, the $CD31Lo/(UEA\text{-}I)^{-}$ population gave rise to both $(UEA\text{-}I)^{+}$ and $(UEA\text{-}I)^{-}$ cells and $CD31Int/(UEA\text{-}I)^{-}$ ended up with $(UEA\text{-}I)^{+}$ cells. Scale bar, 50 μm.

(N) Placental sections stained with CD34 and osteopontin (OPN) antibodies. Some cells are $CD34^{+}$ OPN^{+} (white arrows). Scale bars, 100 μm (left) and 10 μm (right).

(O) Placental sections stained with CD144 and osteopontin (OPN) antibodies. Arrows indicate $CD144^{+}$ OPN^{+} cells. Some cells are subluminal (red arrows) and some are in luminal (white arrows) position. Scale bars, 100 μm (left) and 10 μm (right).

positive cells reside in intimal positions within vascular structures suggesting that *in vivo*, unlike mesenchymal progenitors, EPCs and bipotent progenitors are in the intima of blood vessels (Figures 5I and 5J).

We next assessed whether the $CD45^{-}CD34^{+}$ populations were in contact with the circulation. Placental fetal arteries were perfused by fluorescein isothiocyanate (FITC)-conjugated *Ulex europaeus* agglutinin I (UEA-I), a lectin that binds specifically to endothelial cells (Figure S6). This would only stain populations of endothelial cells in contact with the lumen of perfused arteries harboring the appropriate glycoprotein and glycolipid chains recognized by the lectin. After perfusion, the placental arteries and the immediate surrounding chorionic tissue were dissected and analyzed by flow cytometry (Figures S6 and 5K). After gating on the $CD45^{-}CD34^{+}$ population, CD31Hi cells were expectedly and entirely UEA-I positive, validating successful labeling of all mature endothelial cells (Figure 5K). On the other hand, CD31Neg cells enriched for mesenchymal progenitors were entirely negative, consistent with the specificity of the lectin labeling. CD31Int cells harboring the EPCs as well as the CD31Lo cells harboring bipotential progenitors had positive and negative fractions (Figure 5K).

We next sorted and cultured each of the six populations described above. Almost all cells in CD31Neg/UEA-INeg cells gave rise to mesenchymal colonies. Even if UEA-I-positive and -negative cells were observed in the CD31Lo population, only the UEA-I-negative cells gave rise to colonies that had the bipotential morphology (Figure 5K). To our surprise and similarly, only CD31Int/UEA-INeg cells could give rise to HPP-ECFCs upon culture (Figure 5K). None of the UEA-I-positive fractions including the CD31Hi population could form proliferative colonies and were restricted to non-proliferating ECs upon culture. In addition, immunofluorescence of placental sections with UEA-I showed that only cells in the luminal position had positive staining (Figure 5L).

Of interest, ECFCs derived from the CD31Int/UEA-INeg population could be homogeneously labeled with UEA-I after culturing in EGM2 (Figure 5M), indicating that endogenous EPCs *in vivo* were UEA-1 negative, either because they were not in contact with the circulation or because at a progenitor stage they did not have the lectin binding capacity acquired further in culture. We then stained placental sections using CD144 and osteopontin co-staining (SPP1 or OPN) as identified previously in RNA sequencing (Figure 4). $CD34^{+}OPN^{+}$ or $CD144^{+}OPN^{+}$ cells were in the intima of blood vessels. However, they could be found in either luminal (white arrow) or subluminal (red arrow) positions (Figures 5N and 5O). Overall our experiments indicate that EPCs and bipotent progenitors are derived from the vasculature, and express CD144 do not yet reside in contact with the circulation.

Inhibition of NOTCH Signaling Inhibits Colony Establishment from Meso-Endothelial Progenitors and EPCs

Gene expression analysis suggested that NOTCH signaling may be involved in lineage determination of $CD45^{-}CD34^{+}$ cells. We recently reported the important role of NOTCH signaling in self-renewal of HPP-ECFCs *in vitro* (Patel et al., 2016b; Shafiee et al., 2016). To evaluate the role of NOTCH signaling in the lineage determination of placental populations *in vivo*, we cultured sorted cells in the presence of the γ-secretase inhibitor DAPT in EGM2 (Figure 6A). As expected, colony formation and cell growth for the CD31Neg population was unaffected compared with the control group (DMSO treated) (Figure 6B). Of interest, neither the CD31Lo nor CD31Int population was able to grow in the presence of DAPT despite the establishment of colonies. Compared with controls, these colonies could not be passaged. This provided the indication that NOTCH pathway is activated as supported by RNA sequencing data. Notch plays an essential role in bipotential and EPC populations *in vivo*, as the growth of colonies from CD31Lo, CD31Int populations was severely inhibited (Figure 6B, results from three independent placentas). This was further confirmed through staining of HEY1 and NOTCH1 that displayed an intranuclear localization in EPC and meso-endothelial colonies (Figures 6C and 6D). Finally, pharmacological inhibition of the NOTCH pathway had no effect on the CD31Hi population compared with control. Altogether, inhibition of NOTCH signaling using DAPT counteracts the bipotential and EPC populations, yet had no effect of mesenchymal progenitors and mature endothelial cells.

Differentiation of Meso-Endothelial Bipotent Cells to Mesenchymal Lineage Is Not Mediated by Transforming Growth Factor β1

Compared with CD31Int cells, bipotential CD31Lo cells expressed genes suggestive of activated transforming growth factor β (TGFβ)/bone morphogenetic protein pathway (SCUBE3 and Gremlin). We therefore hypothesized that CD31Lo cells can give rise to mesenchymal lineages through TGFβ1-driven endothelial-to-mesenchymal transdifferentiation (EndMT). To address this hypothesis, we cultured $CD45^{-}CD34^{+}$ subpopulations with TGFβ inhibitor or DMSO after cell sorting and investigated their progeny (Figure 7A). The characteristics of $CD45^{-}CD34^{+}$ subpopulations were not affected in the DMSO-treated group (Figure 7B). Addition of SB431542, an inhibitor of the TGFβ1 receptor activity (James et al., 2010), did not inhibit the growth of CD31Neg, Low, or Int populations (Figure 7C). Culture in the presence of SB431542 resulted in formation of endothelial and mesenchymal cells in the CD31Lo population as expected. Additional formation of

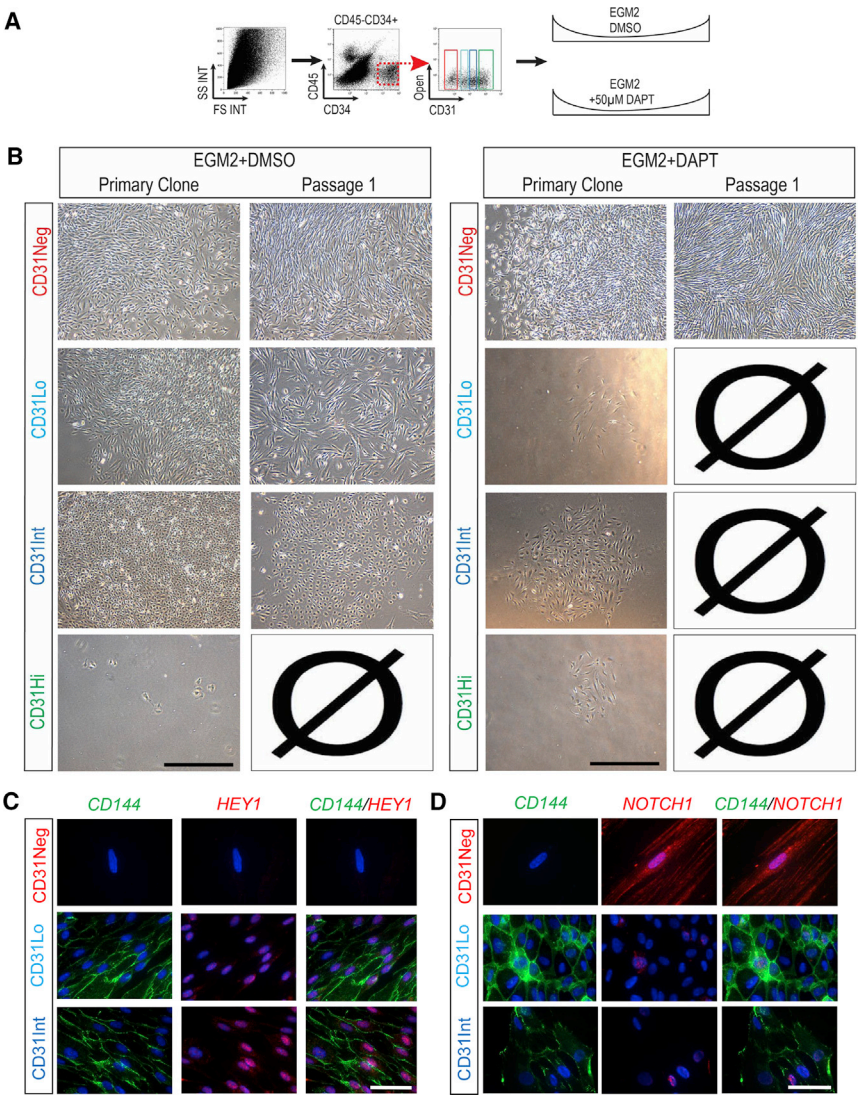

Figure 6. Inhibition of NOTCH Signaling Counteracts Meso-Endothelial Bipotent and Endothelial Progenitor Cell Growth

(A) Placental cells were sorted and cultured in the presence of the γ-secretase inhibitor (DAPT, 50 μM) or DMSO (control group) in endothelial growth medium (EGM2).

(B) Neither CD31Lo nor CD31Int population grew in the presence of DAPT, while culture in DMSO resulted in meso-endothelial bipotent cells (CD31Lo) and EPC (CD31Int) colonies in passage 1.

(C and D) Placental cells were sorted and cultured in the culture slides for 2 weeks and the primary colonies were stained for CD144 and HEY 1 (C) or CD144 and NOTCH1 (D) antibodies.

Scale bars, 100 μm (A and B) and 20 μm (C and D).

ECFCs in the CD31Int population was not affected compared with the control group (DMSO treated) in primary culture. Of interest, TGFβ pathway inhibition increased the level of colony-formation capacity in the CD31Lo population compared with the control group (8,577 ± 996 compared with 3,395 ± 1,950 in 10^6 seeded cells, respectively; not significant, results from three independent placentas, Figure 7D). Addition of SB431542 to the CD31Lo population had no effect on expression of endothelial genes (*PECAM-1*, *CD34*, and *CD144*) compared with the CD31Int population (Figure 7E). Altogether, these findings suggest that the formation of mesenchymal cells from the bipotential population is not mediated through a classical EndMT pathway. This was further confirmed through staining of placental sections for CD31 and SNAIL/SLUG antibodies. Immunohistochemistry showed no expression of SNAIL/SLUG by $CD31^+$ cells (Figure 7F). Immunostaining of primary colonies demonstrated that only the CD31Neg subpopulation expressed SNAIL/SLUG (Figure 7G). Neither EPC nor meso-endothelial colonies stained for SNAIL/SLUG (Figure 7G).

DISCUSSION

Until recently it was postulated that neo-vessel formation in adults is only mediated by angiogenesis. This view has been challenged recently by endothelial precursors being isolated in postnatal life (Asahara et al., 1997; Rafii et al., 1994), although the ontogeny of EPCs is not fully understood. The mesodermal origin of the endothelium allows the hypothesis of the existence of a common bipotent progenitor postdevelopmentally, capable of giving rise to both vasculature and mesenchymal progeny. Here, using a cell

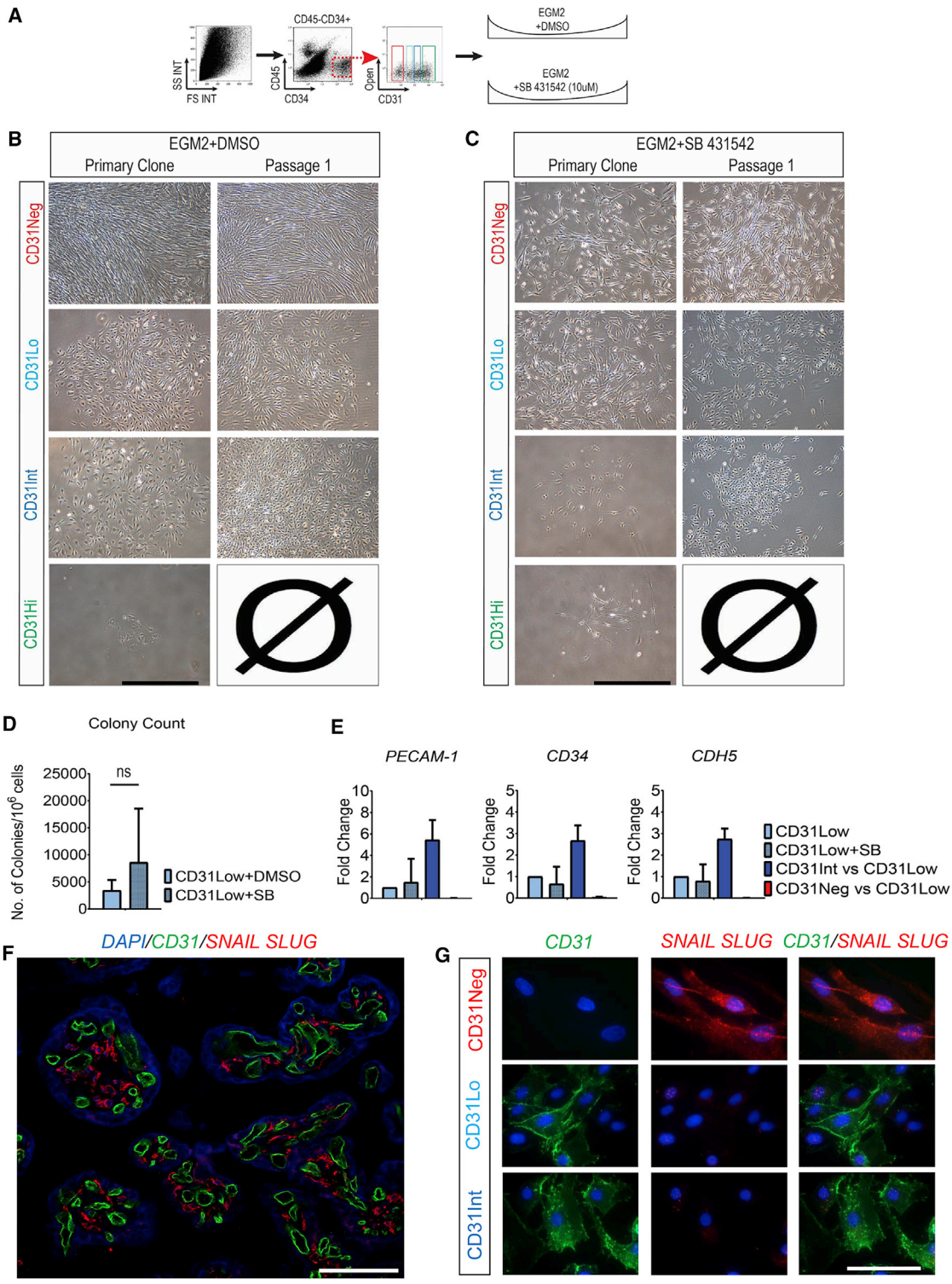

Figure 7. Differentiation of Meso-Endothelial Bipotent Cells to Mesenchymal Lineage Is Not Mediated by the TGFβ Pathway

(A) On sorting, $CD45^{-}CD34^{+}$ subpopulations were cultured with SB431542 (TGFβ inhibitor, 10 μM) or DMSO (control group).

(B) Culture in the presence of SB431542 resulted in bipotential (CD31Lo) and EPC (CD31Int) colonies in passage 1.

(C) Addition of SB431542 did not inhibit the growth of CD31Neg, Low or Int populations in passage 1.

(legend continued on next page)

surface marker based sorting strategy and subsequent colony-forming assays in limiting dilution assays, we have identified *in vivo* a common precursor of mesenchymal and endothelial cells from human term placenta. These bipotential precursors showed differentiation potential to both endothelial and mesenchymal colonies upon culture. Of equal importance, we also identified *in vivo* progenitors that give rise to ECFC colonies. These findings allowed us to decipher the hierarchy between bipotential endothelial progenitors and mature endothelial cells *in vivo*.

Many studies have attempted to identify *in vivo* populations with mesodermal progenitor activity using markers such as c-kit, CD133, and CD45, but most of these markers are also expressed in hematopoietic cells (Case et al., 2007; Hirschi, 2012). We therefore designed a sorting strategy to deplete the $CD45^+$ population. Furthermore, since CD34 has been broadly used as an endothelial progenitor (Case et al., 2007; Peichev et al., 2000) and has provided our previous observations in situations of feto-maternal chimerism (Nassar et al., 2012; Parant et al., 2009), we used the $CD45^-CD34^+$ population as an enriched source of progenitors with endothelial potential. However, culturing the $CD34^+$ population resulted in contaminating mesenchymal cells, as previously reported (Traktuev et al., 2008). In addition, fetal mesenchymal cells have been reported recently to express $CD34^+$ (reviewed in Sidney et al., 2014), highlighting the need for additional markers such as CD31, CD144, or UEA-I. Precise cell surface markers for mesenchymal progenitors ($CD45^-CD34^+CD31^-CD144^-$ UEA-I^-), EPCs ($CD45^-CD34^+CD31IntCD144^+$UEA-$I^-$), and meso-endothelial bipotent progenitors ($CD45^-CD34^+$ $CD31LoCD144^+$UEA-I^-) were established, while use of CD90, CD105, CD106, and CD146 documented the expected phenotype of endothelial versus mesenchymal potential. Meso-endothelial progenitors described here did not show propensity for expansion in skeletal muscle growth medium, suggesting a significant phenotype difference from previously described cells (Dellavalle et al., 2007; Sampaolesi et al., 2003; Tonlorenzi et al., 2007). However, this could be related to culture conditions whereby bipotential cells isolated from muscle may be more likely to adopt a muscle phenotype. An important finding was the lack of staining of meso-endothelial progenitors and EPCs by UEA-I injected intravascularly. Although we cannot rule out the complete absence of the residues required for this lectin attachment at their stage of differentiation, the most plausible explanation is that these progenitors, despite expressing CD144 (VE-cadherin), are not in contact with the circulation, suggesting they are subintimal. However, further studies are needed to confirm this finding. In contrast, mesenchymal progenitors did not seem to be specifically associated with blood vessels. Expression of CD34 has, however, been associated with a pericyte phenotype rather than a neural crest-derived phenotype (Traktuev et al., 2008) (Supplemental Discussion).

Freshly isolated endothelial cells had significant heterogeneity in their ability to generate colonies. As reported previously (Ingram et al., 2004), this could suggest a hierarchy in self-renewal among endothelial cells within the $CD45^-CD34^+$ cells. Accordingly, the CD31Int population that could form HPP-ECFC may be considered as the progenitor of CD31Hi cells *in vivo* that only formed non-proliferating endothelial clusters. This strongly suggests a hierarchy among endothelial cells *in vivo*, recapitulating similar findings in mice as reported recently by us (Patel et al., 2016a).

In conclusion, our study identifies and defines *in vivo* populations of fetal progenitors that can give rise to endothelial, mesenchymal, or both types of colonies (Figure S7A). The characterization of a bipotent mesenchymal and endothelial progenitor further confirms their importance from not only a developmental biology but also from a regenerative medicine point of view. Of interest, these meso-endothelial bipotent progenitors were closely associated with the vasculature (Figure S7B). Current discovered and characterized cell phenotypes might show great potential to be further explored in regenerative medicine applications for vessel formation.

EXPERIMENTAL PROCEDURES

FACS Analysis

Antibodies used for fluorescence-activated cell sorting (FACS) are detailed in Table S1. Placental tissues were cut and single-cell suspensions prepared as reported previously (Patel et al., 2013, 2014). Single-cell suspensions upon digestion were denoted "unsorted population" and cultured in DMEM (Gibco, USA) supplemented with 10% FBS (Gibco), or in the endothelial cell growth medium (EGM2; Lonza, USA). For removal of hematopoietic populations, unsorted cells were resuspended in ice-cold MACS buffer

(D) TGFβ pathway inhibition increased the level of colony-formation capacity in CD31Lo population compared with the control group (ns, not significant; result from three independent placentas).
(E) qRT-PCR analysis confirmed that expression of endothelial genes (*PECAM-1*, *CD34*, and *CD144*) was not affected in the presence of SB431542 compared with the CD31Int population.
(F) Placental sections were stained for CD31 and SNAIL SLUG markers.
(G) Placental cells were sorted and cultured on the culture slides for 2 weeks, then primary colonies were stained for CD31 and SNAIL SLUG antibodies. Scale bars, 100 μm (B, C, and F) and 20 μm (G).

(PBS [Lonza]/0.5% BSA [Sigma]/2.5 mM EDTA disodium salt [Merck, Darmstadt, Germany]) and incubated in Dynabeads CD45 (Invitrogen, USA) for 20 min and the $CD45^+$ cells depleted by using a magnet (DynaMag-15; Invitrogen). For enrichment of endothelial cells, CD45 cells were incubated in CD34 MicroBeads (Miltenyi Biotech, Germany) for 20 min on ice and then loaded onto a MACS column (25 LS Columns) placed in the magnetic field of an MACS Separator. The final $CD45^-CD34^+$ cells were stained using 7-amino-actinomycin D (7-AAD, dilution 1:40) for exclusion of dead cells and also stained with CD34 (dilution 1:25), CD45 (dilution 1:25), and CD31 (dilution 1:30) antibodies (Table S1) for 20 min at 4°C. Cells were sorted using the FACSAria 11u (BD Biosciences, MA) machine. Upon analysis using a pulse geometry gate, cell doublets were eliminated and the $CD34^+$ Hi $CD45^-$ population was gated and sorted into four populations according to the level of CD31 expression. For culture experiments, populations of interest were sorted directly into 100% FBS and then cultured individually in collagen-coated 48-well plates with EGM-2. On day 14 of culture, colonies were counted, analyzed, and passaged.

Perfusion of Placental Vessels with FITC-Conjugated UEA-I

Upon delivery a portion of the placenta was cut and separated under aseptic conditions. Fetal chorionic and amniotic membranes were removed and placental vessels perfused and washed off three times with Ca^{2+}- and Mg^{2+}-free PBS (Gibco). Cleaned vessels were further infused with 10 mL of UEA-I (1:125 dilution) and incubated at room temperature for 10 min. Finally the arteries were cut, enzymatically digested, and sorted as indicated.

Statistical Analysis

Analyses were performed using GraphPad Prism v6.04 software. Descriptive statistics were provided for mean ± SD. Groups were compared by Student's t tests and one- or two-way ANOVA for parametric variables. A Mann-Whitney U test was used to compare non-parametric variables. p Values of <0.05 were considered statistically significant. Here, data represented by histograms and dot plots are the conclusion of at least three independent samples in triplicate unless specified otherwise.

ACCESSION NUMBERS

The transcriptome data can be accessed at Stemformatics (https://www.stemformatics.org/datasets/search#) with the accession number SRP127770.

SUPPLEMENTAL INFORMATION

Supplemental Information includes Supplemental Results, Supplemental Discussion, Supplemental Experimental Procedures, seven figures, and seven tables and can be found with this article online at https://doi.org/10.1016/j.stemcr.2018.01.011.

AUTHOR CONTRIBUTIONS

K.K. designed the research; A.S. and J.P. performed experiments; A.S., J.P., N.M.F., D.W.H., and K.K. analyzed results; A.S., J.P., and K.K. wrote the manuscript; all authors reviewed the manuscript.

ACKNOWLEDGMENTS

This study was supported by the National Health and Medical Research Council (project grant 1023368). K.K. was supported by the National Health and Medical Research Council Career Development Fellowship (grant 1023371). The authors thank Paula Hall and Grace Chojnowski at the QIMR Berghofer Flow Cytometry Unit for assistance with FACS, Susan Brown and RBWH midwifery staff for assistance with tissue collection, and the mothers who donated their placentas for research. K.K., N.M.F., and J.P. are co-inventors on a patent regarding the placental isolation of ECFC and fPL-MSC.

Received: June 21, 2017
Revised: January 16, 2018
Accepted: January 17, 2018
Published: February 22, 2018

REFERENCES

Asahara, T., Murohara, T., Sullivan, A., Silver, M., van der Zee, R., Li, T., Witzenbichler, B., Schatteman, G., and Isner, J.M. (1997). Isolation of putative progenitor endothelial cells for angiogenesis. Science *275*, 964–966.

Bianco, P., and Cossu, G. (1999). Uno, nessuno e centomila: searching for the identity of mesodermal progenitors. Exp. Cell Res. *251*, 257–263.

Bonfanti, C., Rossi, G., Tedesco, F.S., Giannotta, M., Benedetti, S., Tonlorenzi, R., Antonini, S., Marazzi, G., Dejana, E., and Sassoon, D. (2015). PW1/Peg3 expression regulates key properties that determine mesoangioblast stem cell competence. Nat. Commun. *6*, 6364.

Carmeliet, P. (2000). Mechanisms of angiogenesis and arteriogenesis. Nat. Med. *6*, 389–396.

Case, J., Mead, L.E., Bessler, W.K., Prater, D., White, H.A., Saadatzadeh, M.R., Bhavsar, J.R., Yoder, M.C., Haneline, L.S., and Ingram, D.A. (2007). Human $CD34^+$ $AC133^+$ $VEGFR\text{-}2^+$ cells are not endothelial progenitor cells but distinct, primitive hematopoietic progenitors. Exp. Hematol. *35*, 1109–1118.

Choi, K., Kennedy, M., Kazarov, A., Papadimitriou, J.C., and Keller, G. (1998). A common precursor for hematopoietic and endothelial cells. Development *125*, 725–732.

Cossu, G., and Bianco, P. (2003). Mesoangioblasts—vascular progenitors for extravascular mesodermal tissues. Curr. Opin. Genet. Dev. *13*, 537–542.

Dellavalle, A., Sampaolesi, M., Tonlorenzi, R., Tagliafico, E., Sacchetti, B., Perani, L., Innocenzi, A., Galvez, B.G., Messina, G., and Morosetti, R. (2007). Pericytes of human skeletal muscle are myogenic precursors distinct from satellite cells. Nat. Cell Biol. *9*, 255–267.

Dzierzak, E., and Speck, N.A. (2008). Of lineage and legacy: the development of mammalian hematopoietic stem cells. Nat. Immunol. *9*, 129–136.

Hirschi, K.K. (2012). Hemogenic endothelium during development and beyond. Blood *119*, 4823–4827.

Ingram, D.A., Mead, L.E., Tanaka, H., Meade, V., Fenoglio, A., Mortell, K., Pollok, K., Ferkowicz, M.J., Gilley, D., and Yoder, M.C. (2004). Identification of a novel hierarchy of endothelial progenitor cells using human peripheral and umbilical cord blood. Blood *104*, 2752–2760.

James, D., Nam, H.-S., Seandel, M., Nolan, D., Janovitz, T., Tomishima, M., Studer, L., Lee, G., Lyden, D., and Benezra, R. (2010). Expansion and maintenance of human embryonic stem cell-derived endothelial cells by TGF [beta] inhibition is Id1 dependent. Nat. Biotechnol. *28*, 161–166.

Jiang, Y., Vaessen, B., Lenvik, T., Blackstad, M., Reyes, M., and Verfaillie, C.M. (2002). Multipotent progenitor cells can be isolated from postnatal murine bone marrow, muscle, and brain. Exp. Hematol. *30*, 896–904.

Lietzke, R., and Unsicker, K. (1985). A statistical approach to determine monoclonality after limiting cell plating of a hybridoma clone. J. Immunol. Methods *76*, 223–228.

Minasi, M.G., Riminucci, M., De Angelis, L., Borello, U., Berarducci, B., Innocenzi, A., Caprioli, A., Sirabella, D., Baiocchi, M., and De Maria, R. (2002). The meso-angioblast: a multipotent, self-renewing cell that originates from the dorsal aorta and differentiates into most mesodermal tissues. Development *129*, 2773–2783.

Nassar, D., Droitcourt, C., Mathieu-d'Argent, E., Kim, M.J., Khosrotehrani, K., and Aractingi, S. (2012). Fetal progenitor cells naturally transferred through pregnancy participate in inflammation and angiogenesis during wound healing. FASEB J. *26*, 149–157.

Parant, O., Dubernard, G., Challier, J.-C., Oster, M., Uzan, S., Aractingi, S., and Khosrotehrani, K. (2009). $CD34^+$ cells in maternal placental blood are mainly fetal in origin and express endothelial markers. Lab. Invest. *89*, 915–923.

Pardanaud, L., Luton, D., Prigent, M., Bourcheix, L.-M., Catala, M., and Dieterlen-Lièvre, F. (1996). Two distinct endothelial lineages in ontogeny, one of them related to hemopoiesis. Development *122*, 1363–1371.

Patel, J., Seppanen, E., Chong, M.S., Yeo, J.S., Teo, E.Y., Chan, J.K., Fisk, N.M., and Khosrotehrani, K. (2013). Prospective surface marker-based isolation and expansion of fetal endothelial colony-forming cells from human term placenta. Stem Cells Transl. Med. *2*, 839–847.

Patel, J., Seppanen, E.J., Rodero, M.P., Wong, H.Y., Donovan, P., Neufeld, Z., Fisk, N.M., François, M., and Khosrotehrani, K. (2016a). Functional definition of progenitors versus mature endothelial cells reveals key SoxF-dependent differentiation process. Circulation *135*, 786–805.

Patel, J., Shafiee, A., Wang, W., Fisk, N., and Khosrotehrani, K. (2014). Novel isolation strategy to deliver pure fetal-origin and maternal-origin mesenchymal stem cell (MSC) populations from human term placenta. Placenta *35*, 969–971.

Patel, J., Wong, H.Y., Wang, W., Alexis, J., Shafiee, A., Stevenson, A.J., Gabrielli, B., Fisk, N.M., and Khosrotehrani, K. (2016b). Self-renewal and high proliferative colony forming capacity of late-outgrowth endothelial progenitors is regulated by cyclin-dependent kinase inhibitors driven by notch signaling. Stem Cells *34*, 902–912.

Peichev, M., Naiyer, A.J., Pereira, D., Zhu, Z., Lane, W.J., Williams, M., Oz, M.C., Hicklin, D.J., Witte, L., and Moore, M.A. (2000). Expression of VEGFR-2 and AC133 by circulating human $CD34^+$ cells identifies a population of functional endothelial precursors. Blood *95*, 952–958.

Pittenger, M.F., Mackay, A.M., Beck, S.C., Jaiswal, R.K., Douglas, R., Mosca, J.D., Moorman, M.A., Simonetti, D.W., Craig, S., and Marshak, D.R. (1999). Multilineage potential of adult human mesenchymal stem cells. Science *284*, 143–147.

Rafii, S., Shapiro, F., Rimarachin, J., Nachman, R., Ferris, B., Weksler, B., Moore, M., and Asch, A. (1994). Isolation and characterization of human bone marrow microvascular endothelial cells: hematopoietic progenitor cell adhesion. Blood *84*, 10–19.

Reyes, M., Dudek, A., Jahagirdar, B., Koodie, L., Marker, P.H., and Verfaillie, C.M. (2002). Origin of endothelial progenitors in human postnatal bone marrow. J. Clin. Invest. *109*, 337–346.

Roobrouck, V.D., Clavel, C., Jacobs, S.A., Ulloa-Montoya, F., Crippa, S., Sohni, A., Roberts, S.J., Luyten, F.P., Van Gool, S.W., and Sampaolesi, M. (2011). Differentiation potential of human postnatal mesenchymal stem cells, mesoangioblasts, and multipotent adult progenitor cells reflected in their transcriptome and partially influenced by the culture conditions. Stem Cells *29*, 871–882.

Sampaolesi, M., Torrente, Y., Innocenzi, A., Tonlorenzi, R., D'Antona, G., Pellegrino, M.A., Barresi, R., Bresolin, N., De Angelis, M.G.C., and Campbell, K.P. (2003). Cell therapy of α-sarcoglycan null dystrophic mice through intra-arterial delivery of mesoangioblasts. Science *301*, 487–492.

Shafiee, A., Patel, J., Wong, H.Y., Donovan, P., Hutmacher, D.W., Fisk, N.M., and Khosrotehrani, K. (2017). Priming of endothelial colony-forming cells in a mesenchymal niche improves engraftment and vasculogenic potential by initiating mesenchymal transition orchestrated by NOTCH signaling. FASEB J. *31*, 610–624.

Sidney, L.E., Branch, M.J., Dunphy, S.E., Dua, H.S., and Hopkinson, A. (2014). Concise review: evidence for CD34 as a common marker for diverse progenitors. Stem Cells *32*, 1380–1389.

Tonlorenzi, R., Dellavalle, A., Schnapp, E., Cossu, G., and Sampaolesi, M. (2007). Isolation and characterization of mesoangioblasts from mouse, dog, and human tissues. Curr. Protoc. Stem Cell Biol. *Chapter 2*, Unit 2B.1.

Traktuev, D.O., Merfeld-Clauss, S., Li, J., Kolonin, M., Arap, W., Pasqualini, R., Johnstone, B.H., and March, K.L. (2008). A population of multipotent CD34-positive adipose stromal cells share pericyte and mesenchymal surface markers, reside in a periendothelial location, and stabilize endothelial networks. Circ. Res. *102*, 77–85.

Vodyanik, M.A., Yu, J., Zhang, X., Tian, S., Stewart, R., Thomson, J.A., and Slukvin, I.I. (2010). A mesoderm-derived precursor for mesenchymal stem and endothelial cells. Cell Stem Cell *7*, 718–729.

Yoder, M.C. (2010). Is endothelium the origin of endothelial progenitor cells? Arterioscler. Thromb. Vasc. Biol. *30*, 1094–1103.

Stem Cell Reports, Volume *10*

Supplemental Information

Meso-Endothelial Bipotent Progenitors from Human Placenta Display Distinct Molecular and Cellular Identity

Abbas Shafiee, Jatin Patel, Dietmar W. Hutmacher, Nicholas M. Fisk, and Kiarash Khosrotehrani

Supplemental Information

Title: Meso-Endothelial bipotent progenitors from human placenta display distinct molecular and cellular identity

Authors: Abbas Shafiee, Jatin Patel, Dietmar W. Hutmacher, Nicholas M. Fisk, Kiarash Khosrotehrani.

Supplemental Information List

Supplemental Figures

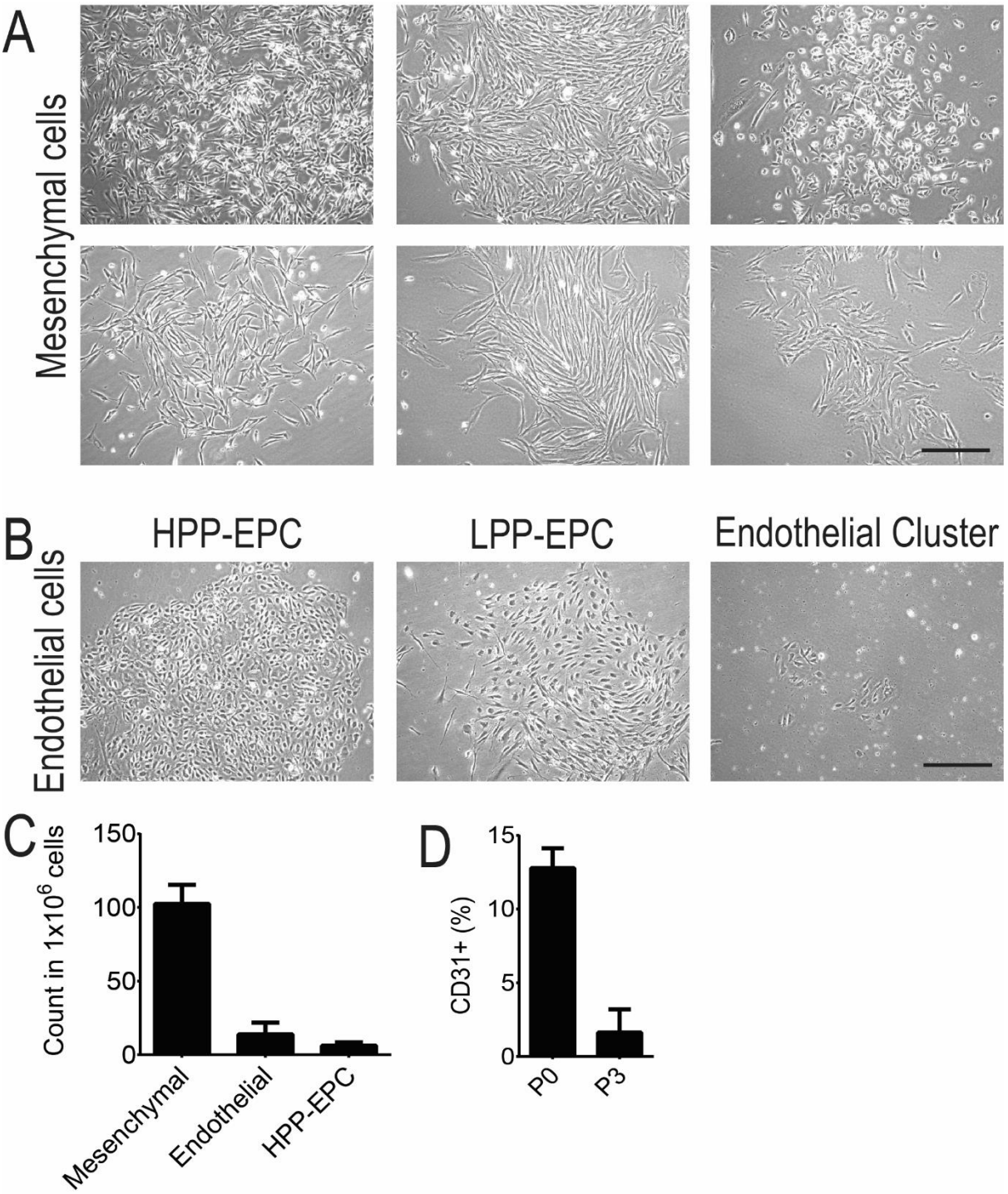

Supplemental Figure 1 (related to Figure 1): Persistent culturing unsorted placental cells resulted in maternal mesenchymal stem cells.

A-B) Unsorted term placental cells were cultured in endothelial growth medium, and this resulted in harvesting both A) mesenchymal and B) endothelial cells, including high proliferative potential-(HPP), low proliferative potential (LPP-) endothelial progenitor cells (EPC) and endothelial clusters at primary culture. C) Placental unsorted population harbours a small HPP-EPC fraction (0.0066 +/- 0.001%). D) Flow cytometry confirmed 12.36 +/- 3.92 (%) of unsorted placental cells could express CD31 at primary culture. Scale bar: 100µm.

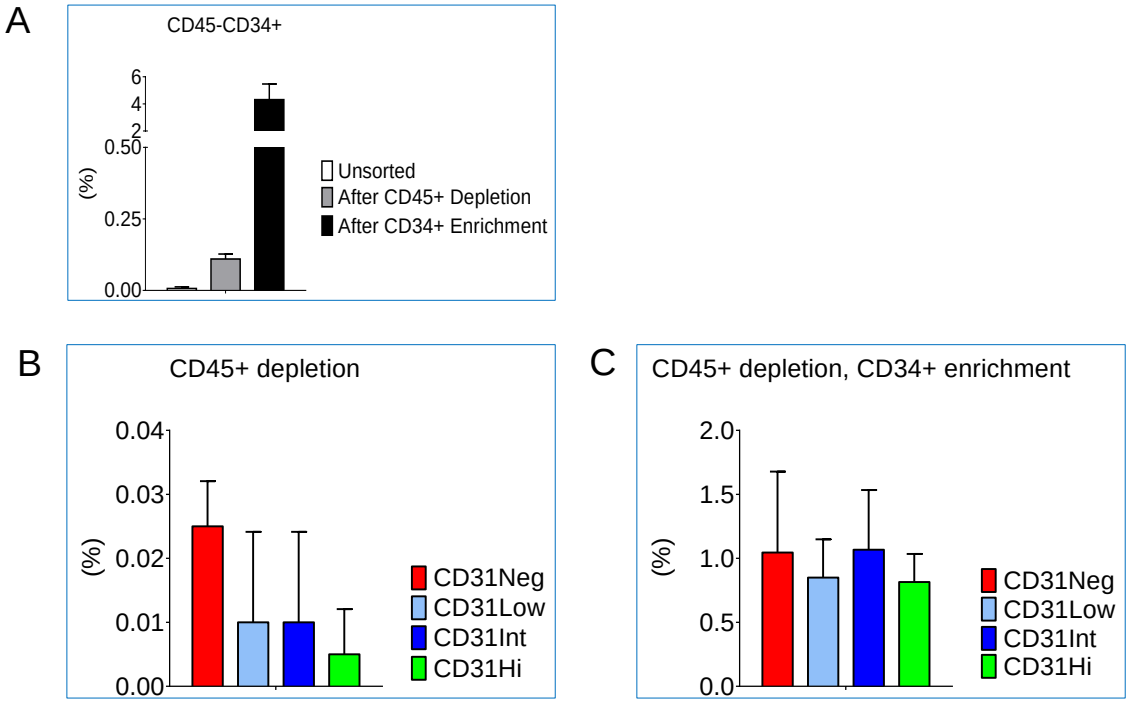

Supplemental Figure 2 (related to Figure 1): The percentage distribution for each subpopulation at each step of sorting. The percentage distribution for each subpopulation was calculated using flow cytometry. A) The percentage of CD45-CD34+ population after CD45+ depletion and CD45+ depletion, CD34+ enrichment. B) The percentage distribution for each subpopulation after CD45+ depletion and CD45+ depletion, CD34+ enrichment. Data presented as mean +/- SD.

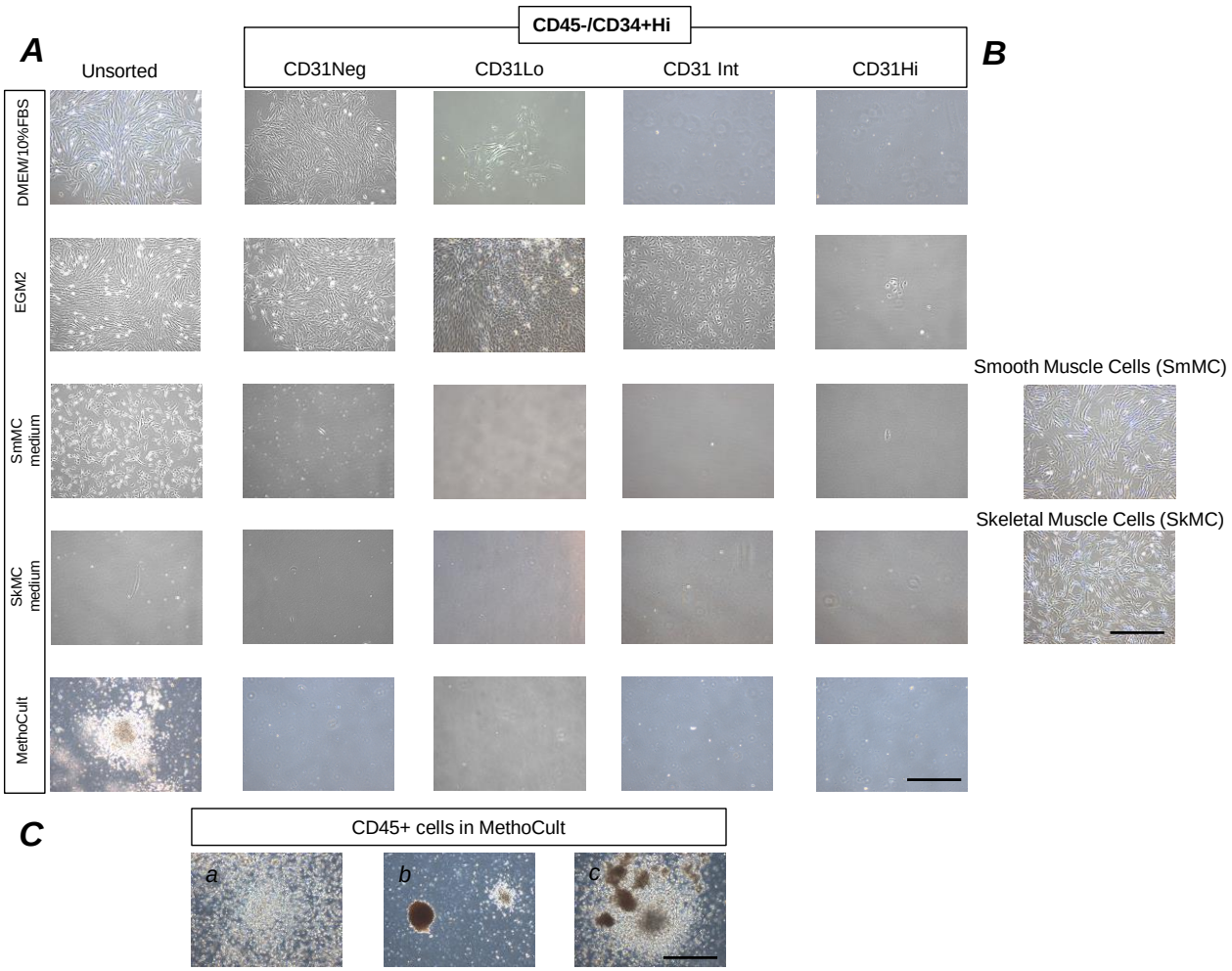

Supplemental Figure 3 (related to Figure 2): Characterization of placenta derived cells. A) Representative images for placental cells cultured in different culture media for 2-3 weeks. Placental cells cultured and monitored for 2-3 weeks. B) Primary skeletal and smooth muscle cells were cultured in their respective growth media. C) Placental CD45+ cells were used as positive control and gave rise to several types of hematopoietic colonies in Methocult, a) CFU-GM colony, b) Two BFU-E colonies one a compact and a small colony, c) A CFU-GM colony and several BFU-E colonies. EGM2: Endothelial growth medium, DMEM: Dulbecco's Modified Eagle Medium, FBS: fetal bovine serum, SmMC: Smooth muscle cell, SkMC: Skeletal muscle cell. Scale bar: 100µm.

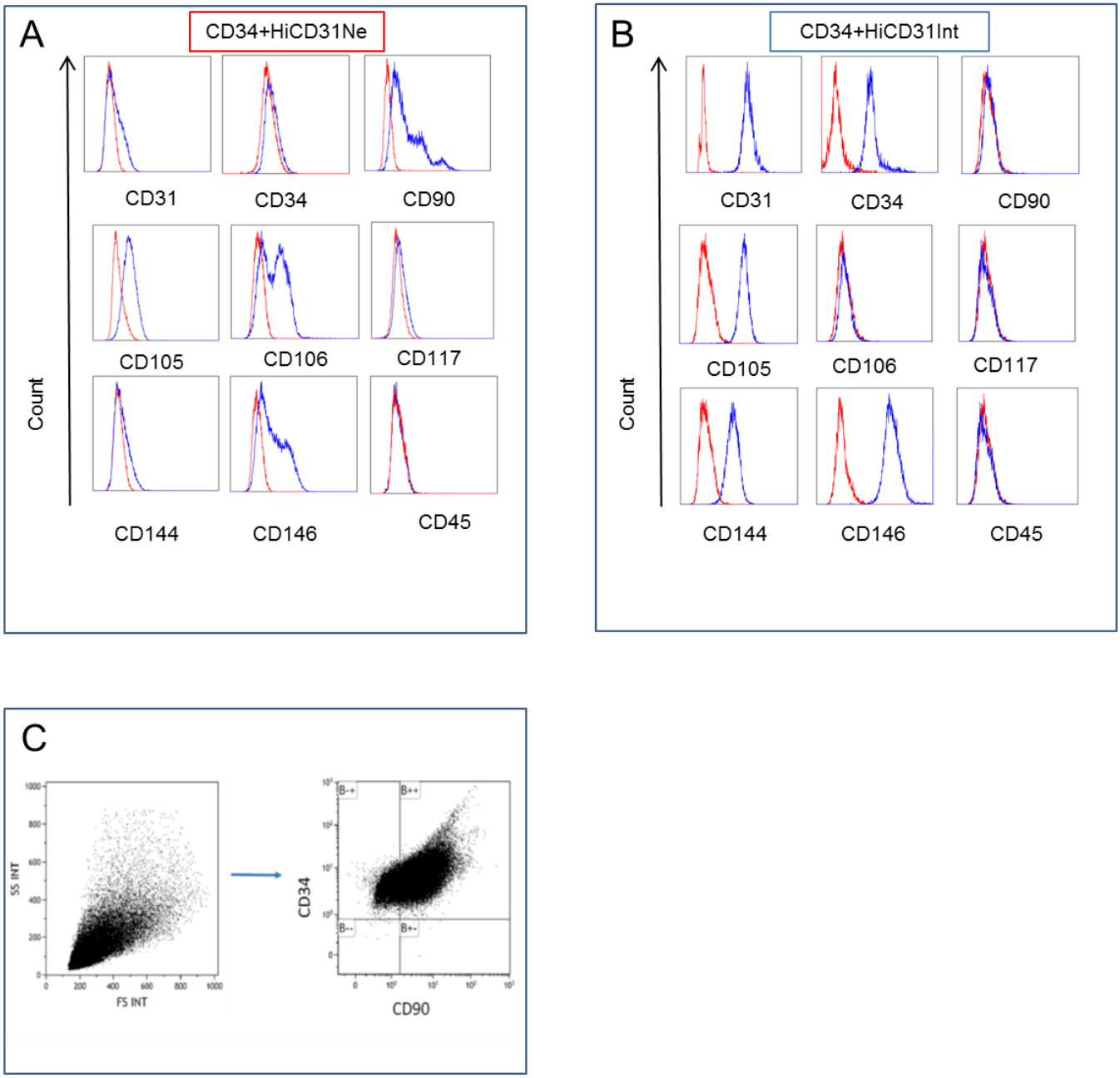

Supplemental Figure 4 (related to Figure 3): CD31Neg and CD31Int derived cells expressed mesenchymal and endothelial key markers respectively.

A) Flow cytometry analysis on colonies isolated from CD31Neg fraction using limiting dilatation assay at passage 1. B) Flow cytometry analysis on colonies isolated from CD31Int fraction using limiting dilution assay at passage 1. C) Dot blot graphs for flow cytometry analysis using multicolor approach (CD34 and CD90 antibodies) for CD31Lo subpopulation.

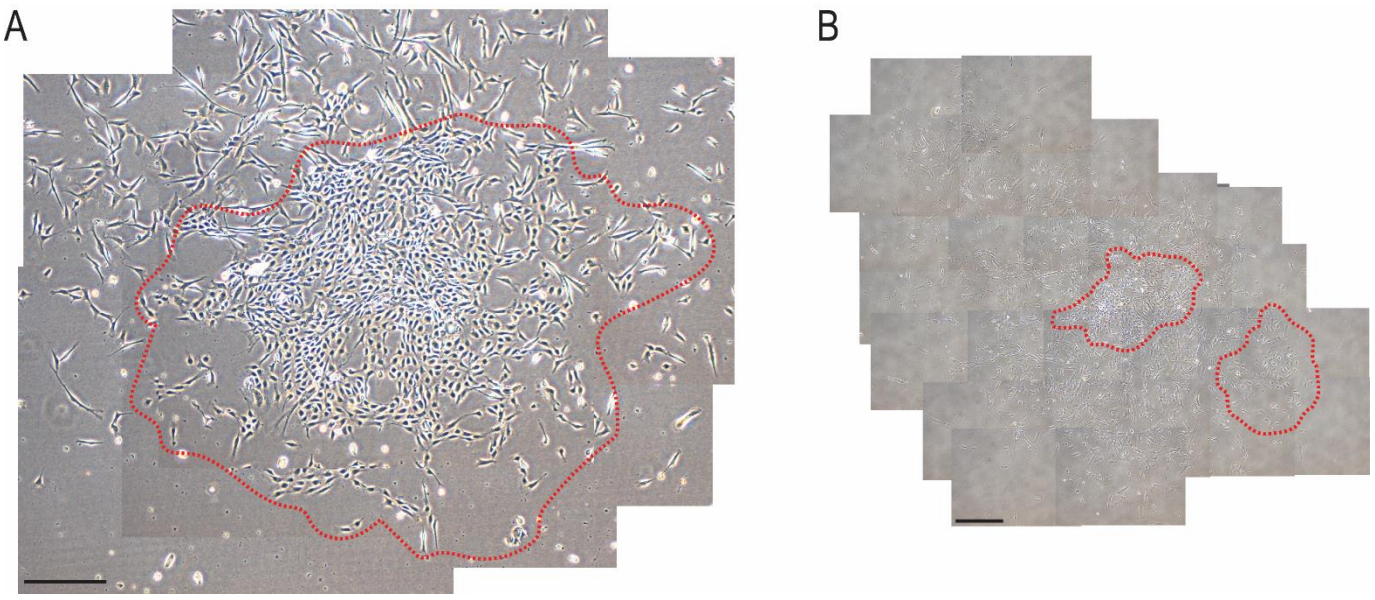

Supplemental Figure 5 (related to Figure 3) A, B) Representative images from CD31Low population at P1 derived from single colony, dashed lines define bipotential colonies surrounded by mesenchymal cells. (Scale bar: 100µm).

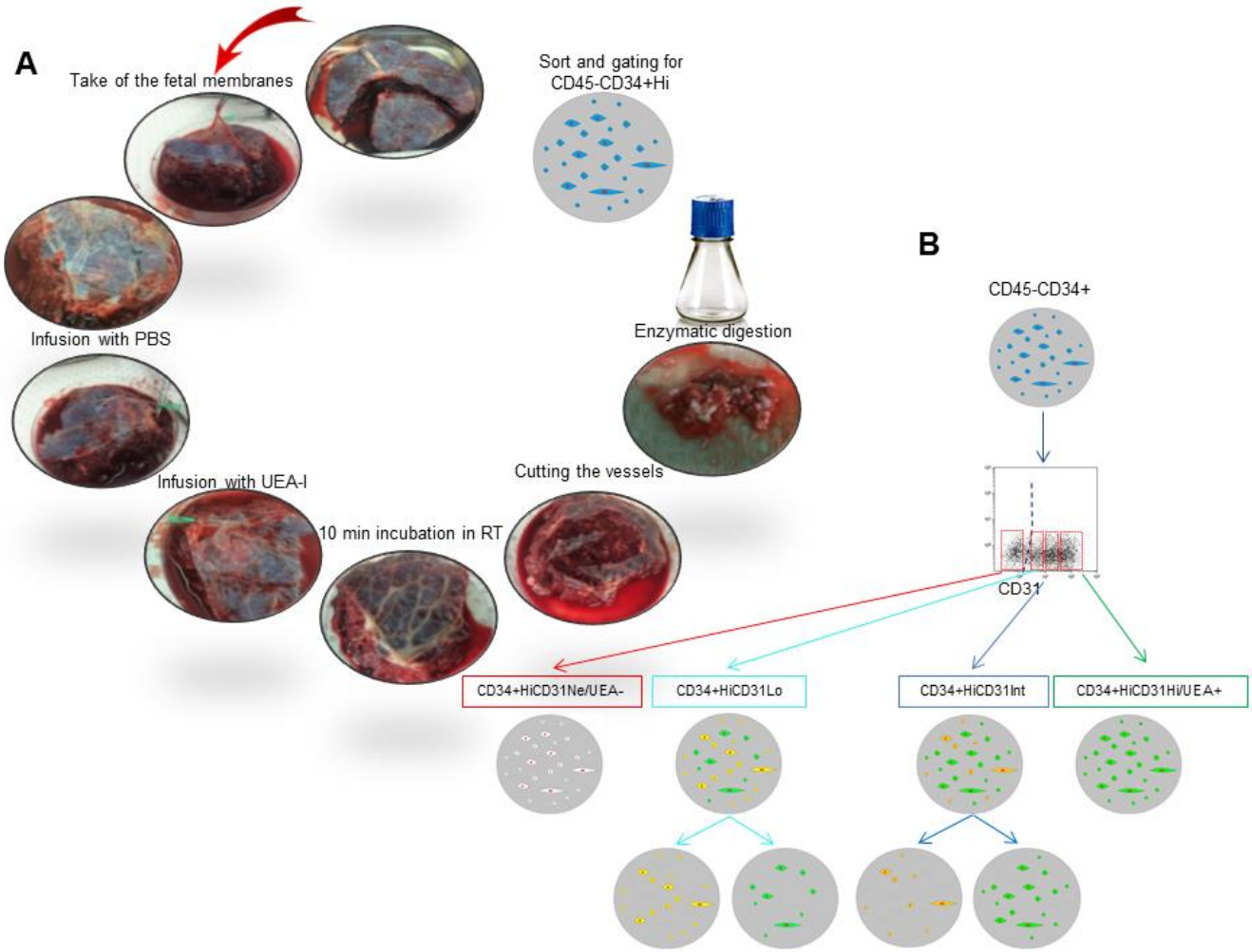

Supplemental Figure 6 (related to Figure 5). Perfusion of fetal placental arteries with FITC-conjugated UEA-I. A) Placental arteries firstly washed off with phosphate buffer saline and then perfused with FITC-conjugated UEA-I. After 10 minutes incubation, arteries were dissected from surrounding chorionic tissue and enzymatically digested and sorted as described. B) Schematic demonstration of CD45-CD34+ population stained for CD31 and UEA-I antibodies.

A

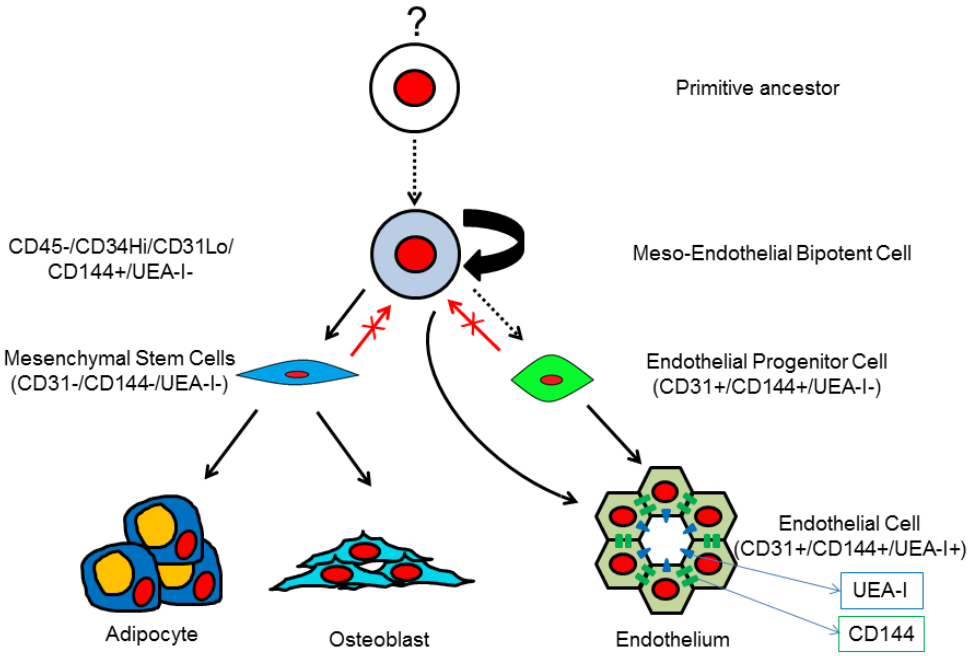
?
Primitive ancestor
CD45-/CD34Hi/CD31Lo/
CD144+/UEA-I-
Meso-Endothelial Bipotent Cell
Mesenchymal Stem Cells
(CD31-/CD144-/UEA-I-)
Endothelial Progenitor Cell
(CD31+/CD144+/UEA-I-)
Endothelial Cell
(CD31+/CD144+/UEA-I+)
UEA-I
CD144
Adipocyte
Osteoblast
Endothelium

B

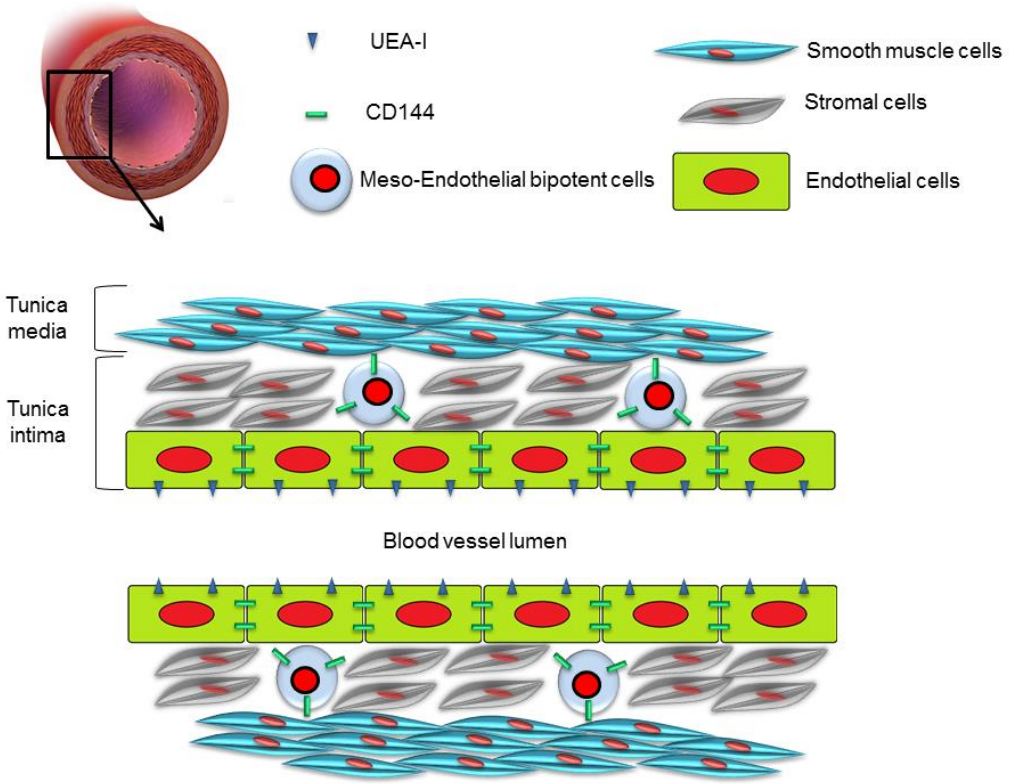
UEA-I
CD144
Meso-Endothelial bipotent cells
Smooth muscle cells
Stromal cells
Endothelial cells
Tunica
media
Tunica
intima
Blood vessel lumen

Supplemental Figure 7 (related Figures 3, 4 and 5). A) Schematic image demonstrating an *in vivo* populations of foetal progenitors (Meso-Endothelial bipotent cell) that can give rise to endothelial, mesenchymal or both types of colonies. B) Schematic image demonstrating that the Meso-Endothelial bipotent progenitors are closely associated with the vasculature but not in contact with the circulation.

Supplemental Tables

Antibody	**Company/Catalogue No**
anti human CD31-V450	BD Biosciences (561653)
anti human CD34-phycoerythrin (PE)	AbD Serotec (MCA1578PE)
anti human CD45-fluorescein isothiocyanate (FITC)	Bio-Legend (304006)
anti human CD45-PE/CY7	Bio-Legend (304016)
anti human CD73-APC	BD Biosciences (560847)
anti human CD90-FITC	BD Biosciences (MCA90F)
anti human CD105-FITC	BD Biosciences (560839)
anti human CD106-FITC	AbD Serotec (MCA907F)
anti human CD117-PE	Abcam (12-1179)
anti human CD146-FITC	BD Biosciences (MCA2141F)
anti human CD144-FITC	BD Biosciences (560411)
7-amino-actinomycin D (7-AAD)	BD Biosciences (559925)

Supplemental Table 1 (related to Figures 1-7). Antibodies used for flow cytometry and FACS.

Endothelial Growth Medium-2 (EGM™-2 Medium)			
Company	Cat. No.	Product	Supplements
Lonza	CC-4176	EGM™-2 SingleQuots™ Kit	Epidermal Growth Factor, Vascular Endothelial Growth Factor, R3-Insulin-like Growth Factor-1, Ascorbic Acid, Hydrocortisone, Fibroblast Growth Factor-Beta, Heparin, Fetal Bovine Serum, Gentamicin/Amphotericin-B, EBM™-2 (Basal Medium).
Mesenchymal Stem Cell Medium			
Gibco	11995073	Dulbecco's modified Eagle's medium (DMEM)	Fetal Bovine Serum, L-Glutamine, High glucose, Pyruvate
Smooth Muscle Cell Medium			
Promocell	C-39262	Smooth Muscle Cell Growth Medium 2	Fetal Calf Serum, Epidermal Growth Factor, Basic Fibroblast Growth Factor, Insulin, Smooth Muscle Cell Basal Medium 2.
Skeletal Muscle Cell Medium			
Promocell	C-39360	Skeletal Muscle Cell Growth Medium	Fetal Calf Serum, Fetuin, Epidermal Growth Factor, Basic Fibroblast Growth Factor, Insulin, Dexamethasone, Skeletal Muscle Cell Basal Medium.
MethoCult™			
Stemcell technology	H4034	MethoCult™ H4034 Optimum	Methylcellulose in Iscove's MDM Fetal Bovine Serum Bovine Serum Albumin 2-Mercaptoethanol Stem Cell Factor GM-CSF G-CSF IL-3 Erythropoietin Other Supplements

Supplemental Table 2 (related to Figure 2). Specific media used to assess lineage differentiation potential.

Primary Antibodies		
Antibody	**Company/Catalogue No**	**Dilution**
anti-human CD34	BD Biosciences, USA (MCA1578PE)	(1:250)
anti-human CD144	BD Biosciences, USA (560411)	(1:200)
anti-human CD31	BD Biosciences, USA (561653)	(1:250)
anti-human CD146	EBioscience, USA (MCA2141F)	(1:200)
anti-human CD45	Biolegend, USA (304016)	(1:200)
anti-human Vimentin	Abcam, USA (ab24525)	(1:200)
anti-human alpha smooth muscle Actin(α-SMA)	Abcam, USA (ab5694)	(1:200)
FITC–conjugated Ulex europaeus agglutinin I (UEA-I)	Vector Laboratories, USA (B-1065)	(1:100)
anti-human fibroblast surface protein1 (FSP1)	Abcam, USA (ab11333)	(1:100)
Anti-HEY1	Abcam, USA (ab154077)	(1:200)
Anti-NOTCH1	Abcam, USA (ab52627)	(1:200)
Secondary Antibodies		
Alexa 488 goat anti-rabbit	Invitrogen, USA (A11034)	(1:1,000)
Alexa 488 goat anti-mouse	Invitrogen, USA (A11029)	(1:1,000)
Alexa 568 goat anti-rabbit	Invitrogen, USA (A11036)	(1:1,000)
Alexa 568 goat anti-rat	Invitrogen, USA (A11077)	(1:1,000)
Alexa 568 goat anti-mouse	Invitrogen, USA (A11004)	(1:1,000)

Supplemental Table 3 (related to figures 2, 3, 5, and 6). List of antibodies used for immunohistochemistry and immunocytochemistry.

A)

Primer	Forward (5'-3')	Reverse (5'-3')
CD34	CCTAAGTGACATCAAGGCAGAA	GCACAGCTGGAGGTCTTATT
CD31	TTGGCGGTGGGAAGCTTAC	GCTCTCTGTTAGTCTGCATCTC
CD144	AAGCGTGAGTCGCAAGAATG	TCTCCAGGTTTTCGCCAGTG
ACTA2	AAAAGACAGCTACGTGGGTGA	GCCATGTTCTATCGGGTACTTC
PDGFRB	AGCACCTTCGTTCTGACCTG	TATTCTCCCGTGTCTAGCCCA
HES1	GTCAACACGACACCGGATAA	TTCAGCTGGCTCAGACTTTC
HEY1	TGGAGAGGCGCCGCTGTAGTTA	CAAGGGCGTGCGCGTCAAAGTA
RUNX2	TGGTTACTGTCATGGCGGGTA	TCTCAGATCGTTGAACCTTGCTA
THY1	ATCGCTCTCCTGCTAACAGTC	CTCGTACTGGATGGGTGAACT
GREM2	ATCCCCTCGCCTTACAAGGA	TCTTGCACCAGTCACTCTTGA
SCUBE3	CAGAACACCCCGAGGTCATAC	GCCAGGGATGTTGACACAGTC
SPP1	GAAGTTTCGCAGACCTGACAT	GTATGCACCATTCAACTCCTCG
SOX9	AGCGAACGCACATCAAGAC	CTGTAGGCGATCTGTTGGGG
SOX17	GTGGACCGCACGGAATTTG	GGAGATTCACACCGGAGTCA
MUC12	CCAGTTCAAGCGACCCTTTTA	CGCTGTGGGATACTGTTGATT
DES	TCGGCTCTAAGGGCTCCTC	CGTGGTCAGAAACTCCTGGTT
CSPG4	AGGACGAAGGAACCCTAGAGT	CACAGGCACACTGTTGTGGA
GAPDH	GGTGAAGGTCGGAGT	CAAAGTTGTCATGGA

B)

	CSPG4			*MUC12*		
Population	CD31Neg	CD31Low	CD31Int	CD31Neg	CD31Low	CD31Int
Placenta 1	+	-	-	+	-	-
Placenta 2	+	-	-	+	-	-
Placenta 3	+	-	-	+	-	-

Supplemental Table 4 (related to Figure 4): A) Sequence of primers used for qRT-PCR. B) Only CD31Neg population could highly express pericyte key markers, chondroitin sulfate proteoglycan 4 (*CSPG4*) and *MUC12* as confirmed by qRT-PCR.

Supplemental Table 5 (related to Figure 4). List of genes differentially expressed between CD31Neg and CD31Int populations.

Supplemental Table 6 (related to Figure 4). List of genes differentially expressed between CD31Int and CD31Lo populations.

Supplemental Table 7 (related to Figure 4). List of genes differentially expressed between CD31Lo and CD31Neg populations.

Supplemental methods

Ethics statement

Human term placentas were obtained after written informed consent from mothers with term healthy singleton pregnancies undergoing elective caesarean section at the Royal Brisbane and Women's Hospital (RBWH, Brisbane, Queensland). This protocol was approved by Metro North Human Research Ethics Committee and The University of Queensland Ethics Committee.

Immunocytochemistry (ICC) and immunohistochemistry (IHC)

For ICC assay, placental isolated populations at passage 2 were cultured in the Nunc® Lab-Tek® Chamber Slides (Sigma) in EGM2 and then fixed with 1% paraformaldehyde (PFA) for 15 minutes at 4°C and stained with anti-human CD34, vimentin, alpha smooth muscle actin (alpha-SMA), FITC–conjugated Ulex europaeus agglutinin I (UEA-I), CD45, CD31, and CD144 (Supp. Table 3). Slides were incubated for 2 hours with primary antibodies, then washed with PBS/0.5%Tween and incubated with secondary antibodies (Supp. Table 3) at room temperature (RT) for 45 minutes. Finally, slides were washed again with PBS/0.5%Tween and mounted with Prolong Gold reagent with DAPI (Invitrogen, CA) and observed under a Zeiss Axio microscope (Carl Zeiss, Germany).

Expression of CD144, SNAIL/SLUG (Abcam, Cat No: ab63371) Osteopontin (OPN; Abcam; Cat No: ab8448), and UEA-I in placental tissues was assessed using IHC. A piece of fresh placenta was washed with PBS and fixed in 4% PFA for 2h and then immersed in 20% sucrose (Sigma-Aldrich, USA) and finally embedded in Optimum Cutting Medium (OCT, Tissue-Tek, USA). 8-µm cryosections were prepared using a cryostat (Microm, Thermo Fisher, Germany). Slides were washed with PBS and incubated with 10% normal bovine serum for 20 min to block nonspecific binding. Then slides were stained with anti-human CD34 (1:100 dilution), SNAIL/SLUG (1:200), Osteopontin (OPN; 1:400) and CD144 (1:100 dilution) antibodies by standard IHC protocol. In independent experiments slides were stained with FITC–conjugated UEA-I. Finally, slides were mounted in Prolong Gold anti-fade reagent with DAPI and observed under a Zeiss Axio microscope or Nikon A1R confocal (Nikon, Japan).

Differentiation assay

Upon sorting, cells were cultured in EGM2 until passage 3. The media for mesenchymal cells isolated from CD45-CD34+CD31Neg and CD45-CD34+CD31Lo populations at passage 3 were switched to DMEM/10% FBS and when culture reached 85% confluence, media were changed to adipogenic, or osteogenic media as previously described (Chen et al., 2012). After 2 weeks, bone or adipocyte differentiated cells were fixed in 4% PFA at RT, washed and stained with Alizarin Red S (Sigma) or Oil Red O (Sigma) for the detection of mineralization or lipid droplets respectively. Control cells were cultured in DMEM/10% FBS and stained. To calculate the cell number after *in vitro* culture, 1.0 x 10^4 cells from each proliferative potential CD45+CD34+ subpopulation after isolation were flow sorted and cultured in EGM2 and numbers were calculated after 3 weeks.

Limiting dilution clonal analysis of sorted populations

To assess the population's characteristics at single colony level, limiting dilution clonogenic assays were performed. Cells freshly isolated upon flow-sorting were cultured in EGM2 media in the pre-coated collagen type-I 96-well plate with 10 cells per well density allowing single clones to grow. On day 14 of culture, positive wells were observed microscopically (Nikon Instruments, Japan), scored and then passaged for further expansion. Colonies were examined based on morphology and categorized into mesenchymal-like or cobblestone-like (endothelial) colonies. Endothelial colonies with fewer than 50 cells and no proliferation potential on passage were scored as endothelial clusters (EC), while colonies with 50-2000 cells and no proliferation potential were considered low proliferative potential-EPC (LPP-EPC). Lastly, colonies with more than 2000 cells and highly proliferation potential were deemed to be highly proliferative potential-EPC (HPP-ECFC).We calculated the probability of monoclonality (PoM) as previously described for limiting dilution experiments (Lietzke and Unsicker, 1985). PoM was calculated by using following equation:

$$\text{PoM} = \frac{Sln(S)}{S-1}$$

S = proportion of empty wells.

To assess the expression of endothelial and mesenchymal markers on cells at passage 0 using ICC, freshly isolated and sorted populations were cultured in the Nunc® Lab-Tek® Chambers with low confluency in EGM2. After 2 weeks slides were fixed with 1%PFA for 15 minutes at

4°C and stained with anti-UEA-1, CD31, anti-vimentin, anti- fibroblast surface protein1 (FSP), anti-HEY1, and anti-NOTCH 1 antibodies (Supp. Table. 3) as described above.

Flow cytometry

CD45-CD34+ cells upon MACS or cultured cells at different passages were suspended in MACS buffer and stained with following directly conjugated anti-human CD31, CD34, CD45, CD90, CD105 and CD146 antibodies. Samples were incubated for 20 minutes. Then cells were washed twice with MACS buffer, and about 50,000 events were acquired on a Gallios flow cytometer (Beckman Coulter, USA) with Kaluza flow cytometry analysis software (Beckman Coulter).

RNA-sequencing (RNA-seq) and quantitative real-time PCR (q-PCR) analysis

RNA-seq analysis was performed to assess the gene expression signature of isolated placental populations at transcript level Freshly sorted populations were cultured in EGM2 medium for two weeks. Then total RNA from CD45-CD34+CD31Neg, CD45-CD34+CD31Lo and CD45-CD34+CD31Int colonies at passage 0 was extracted using the RNA easy Plus Mini Kit (Qiagen, CA) according to manufacturer's instruction. The quality and quantity of isolated RNA was analysed with Agilent 2100 Bioanalyzer (Agilent Technologies, Mulgrave, Victoria).

RNA-seq libraries were prepared using the manufacturer's instructions followed by sequencing on Illumina's HiSeq 2500 (Illumina, CA) performed at the Garvan Institute (Sydney, Australia). Sequence data were aligned to GRCm38 with STAR (version 2.5.0c). The read counts were measured using the GENCODE gene annotation. Differential gene expression was measured with DESeq2 (Love et al., 2014). Genes with significant expression levels were selected by applied a false discovery rate-adjusted P value cut-off of $P < 0.05$, and a log fold change cut-off of 2.

Validation of differential expression of selected genes was carried out using q-PCR. Total RNA was extracted using the RNA easy Mini Kit and reverse transcribed to cDNA using the Superscript III Reverse Transcription Kit (Invitrogen, Mount Waverley, Australia). qPCR was conducted using 0.5 μM of forward and reverse primers (Supp. Table 4) with FastStart SYBR Green Master-mix per reaction (Roche Applied Sciences, CA) in a ABI 7700 Sequence Detection System with SDS v1.9 software (Applied Biosystems, Foster City, CA). All PCR

samples were run in triplicate from at least 3 independent placentas. GAPDH primers were used as housekeeping gene control.

Growth and proliferation of sorted populations in specified media

In independent experiments, cell sorted populations were cultured in specific media: DMEM with 10% FBS as a popular cell culture medium for MSC culture, (n=3 independent placentas), Smooth Muscle Cell Medium (n=3 independent placentas, Promocell, Germany), or Skeletal Muscle Cell Medium (n=3 independent placentas, Promocell, Germany) (Supp. Table 2). Human primary skeletal muscle (SkMC) and umbilical artery smooth muscle cells (HUASMC) used as positive control were purchased from Promocell (Germany). The hematopoietic capability of each population was also assessed by culturing each population in MethoCult for 2 weeks (n=3 independent placentas, Stem Cell Technologies, Canada) (Supp. Table 2). The $CD45^+$ population harvested from the same placenta served as a positive control for hematopoietic potential evaluation. Fluorescent In Situ Hybridisation (FISH) analysis was applied in male fetus pregnancies to assess the origin of cells as reported in a previous study (Patel et al., 2014).

The immunocytochemistry (ICC) and immunohistochemistry (IHC), differentiation assay, limiting dilution clonal analysis of sorted populations, RNA-sequencing (RNA-seq) and quantitative real-time PCR (q-PCR) analysis, and perfusion of placental vessels with FITC–conjugated UEA-I sections are available at Supplemental Experimental Procedures.

Assessment of NOTCH and transforming growth factor-β (TGF-β) pathway impact on ECFC function

To assess the impact of the NOTCH pathway on different cell's population isolated from placenta, populations were freshly isolated as indicated and incubated with DAPT (*N*-[(3,5-Difluorophenyl)acetyl]-L-alanyl-2-phenyl]glycine-1,1-dimethylethyl ester, Abcam, CA), a well described γ-secretase inhibitor, or DMSO (control). In current study, DAPT with 50μM concentration was used based on recent research in our laboratory as the optimum concentration to block the NOTCH pathway (Shafiee et al., 2016). In two weeks culture in EGM2 with DAPT or DMSO cells were observed under microscope (Nikon Instruments, Japan), scored and then passaged for further expansion. DAPT treatment assay was performed in 3 independent placentas.

For TGF-β pathway analysis, freshly isolated cells were incubated with SB431542 (10 μM), selective inhibitor of the TGF-β type I receptor (James et al., 2010). After two weeks culture in EGM2 with SB431542 or DMSO, cells were observed under the microscope (Nikon Instruments, Japan), scored and then passaged for further expansion, or RNA was harvested for qRT-PCR analysis. Colonies were examined based on morphology and categorized into mesenchymal-like or cobblestone-like (endothelial) colonies. TGF-β pathway assay was performed in 3 independent placentas.

Supplemental Results

Bipotential cells display vascular and mesenchymal molecular signature

In comparison to CD31Neg population, the CD31Int population had significantly higher expression of endothelial markers, VE-cadherin (vascular endothelial cadherin) (*CDH5*, 10.3x), CD31 (*PECAM1*, 9.5x), *CD34* (8.6x), Von Willebrand factor (*VWF*, 7.6x), and Tyrosine kinase with immunoglobulin-like and EGF-like domains 1 (*TIE1*, 7.2x) (Supp. Table 5). Many genes involved in endothelial function were also upregulated in the CD31Int population, such as *ERG1* (9.9x), *SEMA3G* (9.0x), Plasmalemma vesicle associated protein (*PLVAP*, 8.5x), Apelin (*APLN*, 7.4X), *SOX18* (6.8x), *SOX17* (6.6x), and *SEMA6B* (6.6x) (Supp. Table 5). Compared to the CD31Neg population, CD31Lo again displayed higher expression of genes involved in endothelium definition and function, such as *CDH5* (10.0x), *PECAM1* (9.2x), *CD34* (8.4x), *VWF* (6.8x), *TIE1* (6.6x), and Protocadherin-17 (*PCDH17*, 6.5), Protocadherin 12 (*PCDH12*, 5.9x) (Supp. Table 7). Higher expression of top genes was confirmed using qRT-PCR revealing much larger differences.

CD31Neg cells displayed higher expression of MSC markers: smooth muscle alpha (α)-2 actin (*ACTA2*, 2.3x), Runt-related transcription factor 2 (*RUNX2*, 2.2x), and membrane metallo-endopeptidase (*MME*, 4.4x) (Granéli et al., 2014) (Supp. Table 7). In addition, the CD31Neg population expressed high levels of MSC precursor genes(Barberi et al., 2005; Lian et al., 2007): platelet-derived growth factor receptor alpha (*PDGFRA*, 5.1x), *PDGFRB* (2.7x), fibroblast activation protein (*FAP*, 3.1), *WNT5A* (4.4x) (Barberi et al., 2005) and early chondrogenic and osteogenic marker genes Decorin (*DCN*, 6.8x)(Friedl et al., 2007), Lumican (*LUM*, 6.1x) (Friedl et al., 2007), and Inhibin Beta E Subunit (*INHBE*, 6.3x) (Martin et al., 2010) (Supp. Table 7).

Of interest, only CD31Neg population showed highly expressed key pericyte markers: chondroitin sulfate proteoglycan 4 (*CSPG4*) and *MUC12*, as confirmed by RNA-seq and qRT-PCR, *CSPG4* and *MUC12* expressions only were detectable in CD31Neg population (Supp Table 4). However, in comparison to the CD31Neg component, CD31Lo cells displayed higher expression of mesodermal progenitor genes, ISL LIM Homeobox 1(*ISL1*, 5.2x) (Moretti et al., 2006), Mesenchyme Homeobox 2 (*MEOX2* also known as *MOX2*, 9.9x) (Mankoo et al., 1999), Apelin Receptor (*APLNR*, 4.3x) (Vodyanik et al., 2010), and Endomucin (*EMCN*, 9x) (Vodyanik et al., 2010) (Supp. Table 7). We next examined specific pathways that have

previously been shown of importance in determination of progenitor function and the transition from progenitor to differentiated cells in the endothelium compartment(Orlova et al., 2014) (Patel et al., 2016). Of interest, our cell populations displayed differential expression of SOX genes as confirmed using qRT-PCR (Fig 4G).

Supplemental Discussion

During development, both endothelial cells and mesenchymal cells derive from mesodermal progenitors (Pardanaud et al., 1996). Using positive selection of Flk1 cells, Minasi et al. isolated a precursor from E9.5 mouse dorsal aorta which showed potential to differentiate into mesenchymal, blood, and endothelial lineage cells (Minasi et al., 2002). Our findings corroborate these observations in human term placenta. We demonstrated that bipotent progenitors as well as EPCs can be found in vascular structures *in vivo* as demonstrated by their expression of CD144 and through dissection of fetal arteries. A mesodermal progenitor with potential to acquire either a MSC and/or endothelial phenotype has also been characterized using human embryonic stem cells. In colony-forming assays the mesodermal precursors could express MSC markers and had multi-lineage capability upon differentiation including endothelial potential (Vodyanik et al., 2010). Orlova et al. derived functional ECs and pericytes from the same progenitor using human-induced pluripotent stem cells (Orlova et al., 2014). Although, the existence of an equivalent of a mesenchymoangioblast has not been reported *in vivo,* gene expression profiling suggested a lateral plate mesodermal or extra-embryonic mesodermal origin in accordance with our findings in placenta. Furthermore we show that this bipotential population's plasticity can persist in term placenta. Whether this population is similar to mesodermal precursors with endothelial capacity (MAPCs) (Reyes et al., 2002; Roobrouck et al., 2011)or meso-angioblasts isolated from muscle remains to be addressed. Recently, existence of a population with similar surface marker characteristics in adult human adipose stromal vascular tissue has been reported (SundarRaj et al., 2015).

A limitation of our study is the inability to perform fate mapping given the *in vivo* human setting of our experiments. Whether Meso-Endothelial bipotent progenitors give rise to both EPCs and mesenchymal progenitors *in vivo* is supported by their capacity to give rise to both types of colonies generated by each of their monopotent progenitors. It could thus be argued that our data are supportive of a hierarchy of plasticity with Meso-Endothelial progenitors at the top. However, colony formation and self-renewal of these colonies was not as robust as with the other progenitors. Although this may be due to the culture conditions used herein, our results cannot prove a hierarchy or a lineage relationship between bipotent progenitors and EPCs. In particular, we cannot fully rule out endothelial to mesenchymal transition. Indeed, the Meso-Endothelial progenitors entirely differentiated into MSCs after 3 passages. It could however be argued that EndoMT is highly unlikely in EGM2 medium and blocking TGFβ

signalling, known to be important in EndoMT(Birket et al., 2015; James et al., 2010), did not prevent the derivation of mesenchymal cells from bipotent progenitors.

Supplemental Reference

Barberi, T., Willis, L.M., Socci, N.D., and Studer, L. (2005). Derivation of multipotent mesenchymal precursors from human embryonic stem cells. PLoS Med *2*, e161.

Birket, M.J., Ribeiro, M.C., Verkerk, A.O., Ward, D., Leitoguinho, A.R., Den Hartogh, S.C., Orlova, V.V., Devalla, H.D., Schwach, V., and Bellin, M. (2015). Expansion and patterning of cardiovascular progenitors derived from human pluripotent stem cells. Nature biotechnology *33*, 970-979.

Chen, Y.S., Pelekanos, R.A., Ellis, R.L., Horne, R., Wolvetang, E.J., and Fisk, N.M. (2012). Small molecule mesengenic induction of human induced pluripotent stem cells to generate mesenchymal stem/stromal cells. Stem cells translational medicine *1*, 83-95.

Friedl, G., Schmidt, H., Rehak, I., Kostner, G., Schauenstein, K., and Windhager, R. (2007). Undifferentiated human mesenchymal stem cells (hMSCs) are highly sensitive to mechanical strain: transcriptionally controlled early osteo-chondrogenic response in vitro. Osteoarthritis and Cartilage *15*, 1293-1300.

Granéli, C., Thorfve, A., Ruetschi, U., Brisby, H., Thomsen, P., Lindahl, A., and Karlsson, C. (2014). Novel markers of osteogenic and adipogenic differentiation of human bone marrow stromal cells identified using a quantitative proteomics approach. Stem cell research *12*, 153-165.

James, D., Nam, H.-s., Seandel, M., Nolan, D., Janovitz, T., Tomishima, M., Studer, L., Lee, G., Lyden, D., and Benezra, R. (2010). Expansion and maintenance of human embryonic stem cell-derived endothelial cells by TGF [beta] inhibition is Id1 dependent. Nature biotechnology *28*, 161-166.

Lian, Q., Lye, E., Suan Yeo, K., Khia Way Tan, E., Salto-Tellez, M., Liu, T.M., Palanisamy, N., El Oakley, R.M., Lee, E.H., and Lim, B. (2007). Derivation of clinically compliant MSCs from CD105+, CD24− differentiated human ESCs. Stem Cells *25*, 425-436.

Lietzke, R., and Unsicker, K. (1985). A statistical approach to determine monoclonality after limiting cell plating of a hybridoma clone. Journal of immunological methods *76*, 223-228.

Love, M.I., Huber, W., and Anders, S. (2014). Moderated estimation of fold change and dispersion for RNA-seq data with DESeq2. Genome biology *15*, 550.

Mankoo, B.S., Collins, N.S., Ashby, P., Grigorieva, E., Pevny, L.H., Candia, A., Wright, C.V., Rigby, P.W., and Pachnis, V. (1999). Mox2 is a component of the genetic hierarchy controlling limb muscle development. Nature *400*, 69-73.

Martin, S.K., Fitter, S., Bong, L.F., Drew, J.J., Gronthos, S., Shepherd, P.R., and Zannettino, A.C. (2010). NVP-BEZ235, a dual pan class I PI3 kinase and mTOR inhibitor, promotes osteogenic differentiation in human mesenchymal stromal cells. Journal of Bone and Mineral Research *25*, 2126-2137.

Minasi, M.G., Riminucci, M., De Angelis, L., Borello, U., Berarducci, B., Innocenzi, A., Caprioli, A., Sirabella, D., Baiocchi, M., and De Maria, R. (2002). The meso-angioblast: a multipotent, self-renewing cell that originates from the dorsal aorta and differentiates into most mesodermal tissues. Development *129*, 2773-2783.

Moretti, A., Caron, L., Nakano, A., Lam, J.T., Bernshausen, A., Chen, Y., Qyang, Y., Bu, L., Sasaki, M., and Martin-Puig, S. (2006). Multipotent embryonic isl1+ progenitor cells lead to cardiac, smooth muscle, and endothelial cell diversification. Cell *127*, 1151-1165.

Orlova, V.V., Drabsch, Y., Freund, C., Petrus-Reurer, S., van den Hil, F.E., Muenthaisong, S., ten Dijke, P., and Mummery, C.L. (2014). Functionality of Endothelial Cells and Pericytes From Human Pluripotent Stem Cells Demonstrated in Cultured Vascular Plexus and Zebrafish XenograftsSignificance. Arteriosclerosis, thrombosis, and vascular biology *34*, 177-186.

Pardanaud, L., Luton, D., Prigent, M., Bourcheix, L.-M., Catala, M., and Dieterlen-Lièvre, F. (1996). Two distinct endothelial lineages in ontogeny, one of them related to hemopoiesis. Development *122*, 1363-1371.

Patel, J., Shafiee, A., Wang, W., Fisk, N., and Khosrotehrani, K. (2014). Novel isolation strategy to deliver pure fetal-origin and maternal-origin mesenchymal stem cell (MSC) populations from human term placenta. Placenta *35*, 969-971.

Patel, J., Wong, H.Y., Wang, W., Alexis, J., Shafiee, A., Stevenson, A.J., Gabrielli, B., Fisk, N.M., and Khosrotehrani, K. (2016). Self-renewal and high proliferative colony forming capacity of late-

outgrowth endothelial progenitors is regulated by cyclin-dependent kinase inhibitors driven by notch signaling. Stem Cells.
Reyes, M., Dudek, A., Jahagirdar, B., Koodie, L., Marker, P.H., and Verfaillie, C.M. (2002). Origin of endothelial progenitors in human postnatal bone marrow. The Journal of clinical investigation *109*, 337-346.
Roobrouck, V.D., Clavel, C., Jacobs, S.A., Ulloa-Montoya, F., Crippa, S., Sohni, A., Roberts, S.J., Luyten, F.P., Van Gool, S.W., and Sampaolesi, M. (2011). Differentiation potential of human postnatal mesenchymal stem cells, mesoangioblasts, and multipotent adult progenitor cells reflected in their transcriptome and partially influenced by the culture conditions. Stem Cells *29*, 871-882.
Shafiee, A., Patel, J., Wong, H.Y., Donovan, P., Hutmacher, D.W., Fisk, N.M., and Khosrotehrani, K. (2016). Priming of endothelial colony-forming cells in a mesenchymal niche improves engraftment and vasculogenic potential by initiating mesenchymal transition orchestrated by NOTCH signaling. The FASEB Journal, fj. 201600937.
SundarRaj, S., Deshmukh, A., Priya, N., Krishnan, V.S., Cherat, M., and Majumdar, A.S. (2015). Development of a system and method for automated isolation of stromal vascular fraction from adipose tissue lipoaspirate. Stem cells international *2015*.
Vodyanik, M.A., Yu, J., Zhang, X., Tian, S., Stewart, R., Thomson, J.A., and Slukvin, I.I. (2010). A mesoderm-derived precursor for mesenchymal stem and endothelial cells. Cell Stem Cell *7*, 718-729.